Article

Not peer-reviewed version

Comparative Phenotypic and Genomic Analysis of Virulence-Associated Factors of *Burkholderia glumae* and *B. gladioli* Causing Bacterial Panicle Blight in Rice in Bangladesh

Nasir Uddin , Ismam Ahmed Protic , Fahad Khan , Mangal Shahi , Plabon Saha , Hasibul Hasan , Urmi Akter Moon , Muhammad Iqbal Hossain , Rumana Afroje , Shariful Islam , Fahima Huque , David Alvarez-Ponce , Rashidul Islam *

Posted Date: 9 March 2026

doi: 10.20944/preprints202601.1111.v2

Keywords: *Oryza sativa*; toxoflavin; lipase; polygalacturonase; virulence; DS; PCR; phylogenetic analysis

 doi:10.20944/preprints202601.1111.v2

Article

Comparative Phenotypic and Genomic Analysis of Virulence-Associated Factors of *Burkholderia glumae* and *B. gladioli* Causing Bacterial Panicle Blight in Rice in Bangladesh

Nasir Uddin [1,2], Ismam Ahmed Protic [3], Fahad Khan [2], Mangal Shahi [2], Plabon Saha [2], Hasibul Hasan [2], Urmi Akter Moon [2], Muhammad Iqbal Hossain [5], Rumana Afroje [4], Shariful Islam [1], Fahima Huque [1], David Alvarez-Ponce [3] and Rashidul Islam [2,*]

[1] Department of Agricultural Extension (DAE), Dhaka 1215, Bangladesh
[2] Plant Bacteriology and Biotechnology Laboratory, Department of Plant Pathology, Bangladesh Agricultural University, Mymensingh-2202, Bangladesh
[3] Department of Biology, University of Nevada, Reno, USA
[4] Ministry of Public Administration, Bangladesh Secretariat, Dhaka-1000, Bangladesh
[5] Department of Plant Pathology, Patuakhali Science and Technology University, Dumki, Patuakhali-8602, Bangladesh
* Correspondence: rashidul.islam@bau.edu.bd

Abstract

Bacterial panicle blight (BPB) of rice, a disease caused by *Burkholderia glumae* and *B. gladioli*, threatens global rice yields and has recently emerged in Bangladesh. Three hundred BPB-infected samples from 20 Bangladesh districts were analyzed using S-PG medium and *gyrB* PCR amplification, identifying 46 *B. gladioli* and 5 *B. glumae* potential isolates. Twenty of these isolates were chosen for in-depth characterization. Pathogenicity tests identified BD_21g (*B. glumae*) as the most virulent strain, followed by BDBgla132A (*B. gladioli*). Disease severity on rice strongly correlated with onion bulb assays, validating the assay as a rapid virulence-screening tool. Phenotypic characterization of the 20 isolates revealed substantial variation in toxoflavin production, lipase activity, polygalacturonase activity, motility, and type III secretion system. Comparative genomic analysis of virulence-associated genes between BDBgla132A and BD_21g showed high protein sequence identity, particularly in toxoflavin biosynthesis and transport genes, while genes encoding lipase (li*pA*/*lipB*), polygalacturonase (*pehA*/*pehB*), and those involved in motility, displayed moderate to high identity. Both strains retained virulence-related genes that are homologous to those of *B. cepacia* but displayed differential virulence strategies. Retrotranscribed-qPCR revealed significantly higher expression of toxoflavin and lipase-encoding genes in BD_21g compared with BDBgla132A, consistent with its elevated enzymatic activities. Conversely, BD_21g showed reduced expression of pectinolytic and flagellar genes over BDBgla132A, consistent with the enhanced pectinolytic activity and motility observed in BDBgla132A. These findings reveal that BD_21g (*B. glumae*) and BDBgla132A (*B. gladioli*) rely on different virulence strategies to infect rice, providing critical insights for developing targeted BPB management approaches in Bangladesh.

Keywords: *Oryza sativa*; toxoflavin; lipase; polygalacturonase; virulence; DS; PCR; phylogenetic analysis

 doi:10.20944/preprints202601.1111.v2

1. Introduction

Bacterial panicle blight (BPB) of rice has become a critical global threat, severely impacting rice production in many major rice-growing regions [1]. The incidence and economic losses due to BPB are expected to rise with climate change and increasing temperatures [2]. The disease can be caused by two bacteria, *Burkholderia gladioli* and *Burkholderia glumae* [3]. The version of the disease caused by *B. glumae* is one of the most devastating seed-borne bacterial diseases affecting rice production worldwide [4]. In contrast, *B. gladioli* are typically less virulent and not as commonly found as *B. glumae* [3]. *B. glumae* was first identified in Japan in 1956 as the causal agent of rice grain rot and seedling blight [5]. BPB has been subsequently recorded worldwide in all areas that cultivate rice, including Asia, Africa, and Central and South America [2,4,6]. Recent studies in Bangladesh confirmed that *B. gladioli* and *B. glumae* are responsible for significant BPB outbreaks, with *B. gladioli* being the dominant species [1,7]. The disease produces several forms of damage, with grain spotting, rot, and panicle blight being the most significant, and can cause yield losses of up to 75% [3,6]. BPB is characterized by upright, straw-colored panicles with florets displaying a darker base and a distinctive reddish-brown marginal line separating necrotic and healthy tissue. Severely affected panicles undergo grain abortion before kernel filling, resulting in complete loss of grain development. The upright posture of affected panicles, caused by the absence of grain fill, is a key diagnostic feature distinguishing BPB from other rice diseases [3].

Several biochemical, physiological, and pathological techniques have historically been used to identify and characterize plant-pathogenic *Burkholderia* species [8]. Molecular methods, ranging from conventional Polymerase Chain Reaction (PCR) for the detection of *Burkholderia* species in seed lots and infected tissues to real-time quantitative PCR for sensitive pathogen identification and DNA quantification both in culture and *in planta*, represent the most accurate and sensitive approaches for diagnosing BPB pathogens [9–11]. Real-time reverse transcription quantitative PCR (RT-qPCR) is a highly sensitive and effective technique for quantifying bacterial gene expression, and it has been extensively used to investigate the regulation of virulence genes [12].

A variety of virulence factors influence the pathogenicity of *B. glumae* and *B. gladioli*. Toxoflavin, lipase (which is encoded by genes *lipA* and *lipB*), polygalacturonase (encoded by genes *pehA* and *pehB*), flagellar motility, and the Hrp-type III secretion system (T3SS) are essential for virulence [13,14]. *B. glumae* generates the phytotoxin toxoflavin [1,6-dimethylpyrimido[5,4-*e*]-1,2,4-triazine-5,7(1*H*,6*H*)-dione], a yellow pigment that plays a vital role in pathogenicity [15,16]. Toxoflavin biosynthesis in *B. glumae* initiates at temperatures above 30°C and peaks at 37°C [17]. The tox operons, *toxABCDE* and *toxFGHI,* are implicated in toxoflavin biosynthesis and transport, respectively [15]. Toxoflavin biosynthesis is controlled by *quorum sensing* (cell-to-cell communication, allowing bacterial populations to function as multicellular organisms) and N-octanoyl homoserine lactone C8-HSL, which is produced by TofI and detected by the receiver TofR, which facilitates the recruitment of the transcriptional activators ToxJ and ToxR to the relevant promoters of toxoflavin biosynthesis genes [18]. Lipases efficiently hydrolyze triacylglycerols and synthesize acylglycerol esters. Microbial lipases are valuable in industry due to their superior stability, selectivity, and substrate specificity. In *B. glumae*, lipase also contributes to pathogenicity. *LipA* is the primary extracellular lipase and a key virulence factor [19]. LipA stability and activity depend on a second gene, *lipB*, which encodes a lipase-specific foldase essential for obtaining active extracellular LipA and for protecting it from proteolytic degradation [19,20]. Flagella-mediated motility is a key virulence trait in pathogenic bacteria, as it allows them to move toward their target within the host, giving them an advantage during the initial colonization stages [21]. Furthermore, global regulators like H-NS and the cAMP–CAP complex, as well as environmental cues including temperature, osmotic pressure, pH, and quorum-sensing signals, precisely regulate flagellar activity [22,23]. Plant cell walls, which are rich in polysaccharides, serve as a primary barrier against microbial pathogens. In soft-rot enterobacteria and in the wilt pathogen *Ralstonia solanacearum*, secreted pectinolytic enzymes, including endo- and exopolygalacturonases such as PehA and PehB, are key contributors to tissue maceration and disease [24,25]. In *B. cepacia*, the *pehA*-encoded polygalacturonase is involved in the maceration of onion bulbs

 doi:10.20944/preprints202601.1111.v2

[26]. Despite the identification and characterization of the type II-secreted endo-polygalacturonases PehA and PehB in *Burkholderia glumae*, their precise role in disease development remains unclear, likely reflecting functional redundancy [13]. Finally, the Hrp (hypersensitive response and pathogenicity) type III secretion system is essential for the pathogenicity of numerous plant pathogenic bacteria [27]. In specific plant pathogenic bacteria, *hrp* genes play a crucial role in inducing disease in susceptible plants while triggering a hypersensitive response in resistant plants [28].

A comprehensive understanding of toxoflavin biosynthesis, lipase and polygalacturonase enzymatic activities, and flagellar virulence gene regulation in *B. glumae* and *B. gladioli* remains limited. Comparative analysis of homologous gene clusters across both species can enhance knowledge of their pathogenic strategies. Additionally, the prevalence of bacterial panicle blight (BPB) caused by *B. glumae* and *B. gladioli* in rice in Bangladesh is poorly documented, and ongoing environmental changes are facilitating disease spread throughout the country, highlighting the need for focused research. This study characterizes 19 *B. gladioli* and one *B. glumae* isolate across four major rice-growing districts of Bangladesh by integrating phenotypic assays and genomic comparisons. Phenotypic characterization included quantification of toxoflavin, lipase and polygalacturonase activities, and motility, while genomic analyses encompassed BLASTp comparisons and phylogenetic analyses of orthologous regions for toxin biosynthesis (*toxA–R*), lipase (*lipA*/*lipB*), polygalacturonase (*pehA*/*pehB*), motility-related gene clusters (*cheA, cheB, cheD, cheR, cheW, cheY, cheY1, cheZ, flhA, flhB, flhC, flhD, flhG, fliA, fliC, fliD, tsr, motA, motB*). Moreover, the expression levels of 17 key virulence-linked genes, including *toxA–R*, *lipA*/*lipB*, *pehA*/*pehB*, and *flhC*/*flhF*, were quantified by RT-qPCR in two representative highly virulent isolates: BD_21g (*B. glumae*) and BDBgla132A (*B. gladioli*). By correlating phenotypic variation with genomic diversity, we provide novel insights into BPB pathogenicity and lay the groundwork for targeted management strategies in Bangladesh.

2. Materials and Methods

2.1. Sample collection, isolation and molecular identification of Burkholderia strains

Rice fields cultivating different varieties (HYV, hybrid, local) across three seasons (Aus, Aman, Boro) in 20 districts of Bangladesh were surveyed from mid-October 2022 to November 2023 (Table S1) [29,30]. A total of 300 fields (three locations per district, five fields per location) were sampled, and panicles exhibiting typical BPB symptoms were collected [1]. Typical field symptoms of BPB from seedling to panicle stages include long grayish sheath lesions with dark brown to reddish-brown margins (Figure 1A), erect straw-colored panicles with darkened florets (Figure 1B and 1C), and grain abortion resulting in empty panicles (Figure 1D) [3]. From each sample, 1 g of symptomatic rice grains was surface-sterilized by immersion in 70% ethanol for 15 seconds and 3% sodium hypochlorite for 1 minute, and then ground in a mortar [31]. During grinding with a mortar and pestle, 5 ml of water were added [1], and 20 µl of the resulting suspension were streaked onto the selective medium (S-PG) [32]. Isolates were purified by serial dilution and re-plating, and purple colonies were streaked onto King's B agar (KBA) plate [8] for visual assessment of toxoflavin production. Isolates producing a yellow pigment on KBA were selected and further purified as putative *B. gladioli* and *B. glumae*. Pure cultures were stored in King's B broth (KBB) with 30% glycerol at −70°C, and fresh cultures were prepared as needed on KBA plates. For molecular identification, all isolates were grown in nutrient broth at 28°C for 24 hours and harvested by centrifugation, and genomic DNA was extracted using the Promega Genomic DNA Purification Kit (Promega, USA) according to the manufacturer's protocol. The 16S rDNA gene was amplified from *B. gladioli* and *B. glumae* isolates using the universal primers 16SF and 16SR, as described in refs. [29,30]. Gel electrophoresis (1% agarose) confirmed the presence of PCR products with approximate lengths of 1400 bp and 1494 bp, respectively. The *gyrB* gene was amplified using PCR using species-specific primers [9]: the primers glu-FW and glu-RV were employed to identify *B. glumae*, while the primers gla-FW and and gla-RV were used to identify *B. gladioli*. PCR reactions (25 µL) included one µL of genomic DNA (150–200 ng), 12.5 µL of 2×

 doi:10.20944/preprints202601.1111.v2

Promega master mix, one µL of each primer (5 pmol), and 9.5 µL of nuclease-free water, with thermocycling conditions as follows: initial denaturation at 94°C for 2 minutes; 35 cycles of 94°C for 1 minute, 63°C for 1 minute, and 72°C for 1 minute; and a final extension at 72°C for 8 minutes. PCR products (9 µL) were analyzed by electrophoresis on 1.5% agarose gels stained with ethidium bromide, with amplicon sizes of 529 bp and 479 bp confirming the presence of *B. glumae* and *B. gladioli*, respectively, based on expected *gyrB* gene fragment sizes. For the five samples that tested positive for *B. glumae*, were conducted Sanger sequencing on the PCR products and the obtained sequences were used for species identification via BLAST searches [29].

Figure 1. Typical symptoms of bacterial panicle blight (BPB) of rice. (A) Lesion on the sheath, displaying a vertical grayish area with a dark reddish-brown border (arrow). (B, C) Panicle symptoms include straw-colored spikes with florets showing darker basal and reddish-brown marginal lines. (D) Field infections on a susceptible cultivar (*Oryza sativa* L. cv. Horidhan) showing heavily infected panicles that remain erect due to grain abortion.

2.2. Pathogenicity Tests

Nineteen *B. gladioli* isolates and one *B. glumae* isolate were selected for in-depth characterization based on successfully sequence and assemble their whole genomes, as described in refs. [29,30]. Pathogenicity assays were conducted at two different growth stages, the seedling and heading phases, on a susceptible rice variety (*Oryza sativa* L. cv. Horidhan) to determine the virulence of the selected isolates. The assays were conducted following the protocol described in ref. [3] with a few modifications. Seeds of a susceptible rice variety (*Oryza sativa* L. cv. Horidhan) were sown in sterilized soil contained in plastic pots (15 cm diameter) and grown in a greenhouse under controlled conditions. Given the predisposition of BPB to develop at elevated temperatures, all pathogenicity tests were conducted under controlled conditions maintained at a diurnal temperature range of 37–41°C and a relative humidity (RH) of 75–95%. Bacterial isolates were cultured on King's B agar at 30°C for 24 hours. A loopful of bacterial growth was suspended in 9 mL of sterile distilled water, and the cell density was adjusted to an optical density (OD_{600}) of 0.3, corresponding to approximately 10^7–10^8 CFU/mL, using a spectrophotometer. For seedling inoculation, 5 rice plants/replication were selected, and the third leaf sheath was injected with 0.5 mL of the bacterial suspension using sterile 1 mL syringes equipped with BD 23G1 needles. For heading stage inoculation, 10 panicles/replication were sprayed with the same bacterial suspension when approximately 20–30% of the panicle had emerged from the boot. Sterile distilled water was used as a negative control for both inoculation methods. Three independent experimental replicates were conducted per isolate to ensure robust comparisons of disease severity. Disease symptoms on leaf sheath and panicle were evaluated 2- and 4-weeks post inoculation, respectively. Lesions on sheaths and panicles were scored using a four-point categorical disease scale. Disease severity was assessed 7 and 14 days after inoculation. The disease severity was calculated using a 0 to 9 scale as reported in ref. [33], where the scale indicates 0 = no symptoms; 1 = 0.1–10.0% of the panicle affected; 3 = 11–20% of the panicle affected; 5 = 21–30%

 doi:10.20944/preprints202601.1111.v2

of the panicle affected; 7 = 31–60% of the panicle affected; 9 = >61% of the panicle affected. This information was used to calculate the disease severity according to the equation:

$$\text{Disease severity} = \frac{n_0 \times 0 + n_1 \times 1 + n_3 \times 3 + n_5 \times 5 + n_7 \times 7 + n_9 \times 9}{\text{Total of panicles evaluated}},$$

where n_i indicates the number of panicles with each degree of damage (0 to 9). After disease scoring, bacterial strains were reisolated from diseased plants.

2.3. Onion Assay for Pathogenicity Testing

Onion bulbs were obtained from a local store and utilized as a host model to assess pathogenicity. The virulence of *B. gladioli and B. glumae strains* was assessed on onion bulb scales following a modified protocol based on ref. [34]. A 5 µL aliquot of bacterial suspension (approximately 5×10^5 CFU in 10 mM $MgCl_2$) was applied to a ~2 mm incision made on the inner surface of each onion bulb scale using a micropipette tip. The inoculated onion scales were incubated in a humid chamber at 30°C. After 48 hours, virulence was evaluated by measuring the area of tissue maceration at the inoculation site.

2.4. Hypersensitive Response (HR) Assay

Hypersensitive response assays were conducted following the method described in ref. [35] with minor modifications. Tobacco plants (*Nicotiana tabacum* L.) were grown in plastic pots filled with sterile soil under controlled greenhouse conditions with natural daylight and a temperature range of 25–28°C. Bacterial isolates were cultured on potato semi-synthetic agar (PSA) medium prepared with 5 g of peptone, 15 g of sucrose, 2 g of $Na_2HPO_4 \cdot 12H_2O$, 0.5 g of $Ca(NO_3)_2 \cdot 4H_2O$, and 15 g of agar per liter of potato decoction (obtained by boiling 300 g of potatoes in 1 L of distilled water and filtering). The pH was adjusted to 7.0 before autoclaving. Cultures were incubated at 30°C for 48 hours. For infiltration, a loopful of bacterial growth was suspended in 9 mL of sterile distilled water, and the cell suspension was adjusted to an optical density of OD_{600} = 0.3, corresponding to approximately 10^7–10^8 CFU/mL. Using a 1mL hypodermic syringe without a needle, 0.5 mL of the suspension was infiltrated into the intercellular spaces of the fully expanded third and fourth leaves of each plant at the 8th–9th leaf stage. Control plants were infiltrated with sterile distilled water. A small pinprick was made at each infiltration site to ensure uniformity, and one leaf with five infiltration points was used per bacterial strain. Plants were kept in controlled conditions at 37–41°C with a relative humidity of 75–90% during the day, and hypersensitivity was observed post-infiltration after 24, 48 and 72 hours.

2.5. Determination of Toxoflavin Production and Quantitative Analysis

Toxoflavin synthesis was evaluated to compare virulence levels among *B. gladioli* and *B. glumae* strains. Bacterial cells were cultured on King's B (KB) agar plates and incubated at 37°C for 48 h to assess toxoflavin production [8]. Sterile King's B (KB) agar plates without bacterial inoculation were used as the negative control for the toxoflavin production assay. The presence of toxoflavin was determined by the appearance of a bright yellow pigment diffusing from the bacterial colonies into the surrounding agar, which was absent in the sterile control [8]. For a quantitative measurement of the production of toxoflavin, cells were gently removed, and the remaining agar slabs containing diffused toxoflavin were excised with a sterile razor blade into small, ~5×5×5 mm fragments. The chopped agar was mixed with chloroform in a 1:1 (w/v) ratio, vortexed for 5 minutes, incubated at room temperature for 30 minutes for toxoflavin extraction, and the chloroform fraction was filtered through filter paper and collected in a new microtube. Chloroform was evaporated, and the culture filtrate residue was dissolved in 80% methanol as previously described [15]. The absorbance of each sample was measured at 393 nm to determine relative toxoflavin production [36].

 doi:10.20944/preprints202601.1111.v2

2.6. Assessment and Quantitative Evaluation of Lipase activity

To screen for lipolytic bacteria, isolated colonies were inoculated onto agar plates enriched with 1% v/v Tween 20 (Peptone 10 g/L, NaCl 5 g/L, $CaCl_2 \cdot 2H_2O$ 0.1 g/L, agar 15 g/L, pH 7.4), alongside sterile uninoculated Tween 20 agar plates as negative controls, and incubated at 30 °C for 24 hours [37]. The presence of opaque halos surrounding the colonies, which were absent in sterile controls, indicated lipase activity [37]. Lipase activity was quantified using the method described in ref. [38], modified as follows. Overnight cultures grown at optimal temperature (37°C) in LB broth with shaking (200 rpm) were centrifuged at 13,000 rpm for 10 minutes. A substrate solution was prepared by dissolving 75 mg of p-nitrophenyl palmitate in 10 mL of isopropanol and dissolving it in 90 mL of 0.05 M Sorensen's phosphate buffer, pH 8.0, containing 207 mg of sodium deoxycholate, 50 mg of gum Arabic, and pre-warming solution. For the assays, 0.1 mL of cell-free supernatant was incubated at 37°C for 15 minutes with 2.4 mL of pre-warmed substrate alongside substrate-only blanks as negative controls. Lipase activity was detected as a bright yellow color, produced by p-nitrophenol, and the absorbance at 410 nm was measured using a spectrophotometer.

2.7. Qualitative and Quantitative Analysis of Polygalacturonase Activity

Polygalacturonase activity was observed in the semi-solid pectate-yeast extract agar (PEC-YA) medium [39] prepared with slight modifications. Polygalacturonase activity was observed in the semi-solid pectate-yeast extract agar (PEC-YA) medium prepared with slight modifications, alongside sterile uninoculated PEC-YA plates as negative controls. The medium was prepared in a 1 L Erlenmeyer flask containing 6.4×10^{-4} N NaOH, 1.5 g agar, 100 mL cold distilled water, 1 g yeast extract powder (Difco), 1 mL bromothymol blue, and 1 g polygalacturonic acid. This medium was rapidly stirred and heated until complete dissolution. After dissolving, the pH was adjusted to ~7.3 (checked with bromothymol blue and pH paper), and was sterilized in an autoclave for 15 min at 121°C. After cooling the broth to 50°C, it was poured into sterile Petri dishes. Bacterial cultures were spotted onto the plates and incubated at 30°C. A halo of clear color was visible around the colonies when the plate was flooded with 2N HCl, indicating that polygalacturonase degraded polygalacturonic acid; the halo, however, was absent in the negative control. For quantitative analysis, bacterial isolates were grown in M9 minimal medium [40] supplemented with 0.3% of citric acid and 0.2% of PGA at pH 5.2 and 30°C for 48 h with shaking at 180 rpm. The supernatant caused by centrifugation (10,000 × g, 10 min) of the culture was incubated with a mixture of 0.5% of PGA and 50 mM sodium acetate buffer, pH 3.5, at 37°C for 30 min. The reaction was stopped by adding 500 µL of Bernfeld reagent [41] (1% 3,5-dinitrosalicylic acid, 5.3 M potassium sodium tartrate, 2 M NaOH). The mixture was then boiled for 10 min, cooled, and the absorbance was measured at 530 nm.

2.8. Bacterial swarming motility assay

This experiment was conducted utilizing LB broth in agar at a concentration of 0.5% (w/v). Each strain was incubated at 30°C for 12 to 14 hours in 2 mL of LB liquid medium. Subsequently, 1 mL of cultured cells was pelleted by centrifugation at 900 × g for 2 minutes. The collected cells were rinsed with 1 mL of new LB liquid media, and the centrifugation process was repeated. The washed pellet was resuspended in 100 µL of distilled water, and one µL of the solution was spotted onto the center of a swarming agar plate. The assay plate was incubated at 30°C for 24 hours [42]. Sterile uninoculated LB agar plates were prepared and incubated under identical conditions as negative control. Each strain was tested in five biological replicates, and the experiment was independently repeated three times to confirm reproducibility.

2.9. Transcript Level Determination

Total RNA was extracted from *Burkholderia* strains using the SV Total RNA Isolation System (Promega, Madison, WI, USA). Overnight cultures were prepared by growing bacteria in 5 mL of King's B medium at 32°C with shaking at 180 rpm. These were diluted 1:50 into fresh King's B

 doi:10.20944/preprints202601.1111.v2

medium, and 10 mL were subcultured until reaching the late exponential to early stationary phase (OD_{600} ≈ 1.5). A 1 mL aliquot was harvested by centrifugation, and total RNA was isolated according to the manufacturer's instructions. Residual genomic DNA was removed by RNase-free DNase I treatment, and DNA contamination was excluded by PCR using gene-specific primers on RNA samples without reverse transcriptase. Complementary DNA (cDNA) was synthesized using 250 ng of RNA per reaction with the GoScript Reverse Transcription System (Promega), following the manufacturer's protocol. For quality control, parallel reactions omitting reverse transcriptase were included to confirm the absence of DNA. Quantitative real-time PCR (qPCR) was conducted using the Bio-Rad Real-Time PCR system with Power SYBR® Green PCR Master Mix (Promega, USA). Amplification conditions included an initial denaturation at 95°C for 3 minutes, followed by 40 cycles of 95°C for 1 minute and 55°C for 1 minute. Melting curve analysis was performed by heating to 65°C for 30 seconds. Transcript levels of virulence-associated genes, including *toxA–R*, *lipA/lipB*, *pehA/pehB*, *flhC*, and *flhF*, were quantified using the ΔΔCT method [43] with 16S rRNA serving as the internal reference. Primers were designed using BLAST searches against the *B. glumae* reference genome BGR1 (GCF_000022645.2) and are shown in Table S2. ΔCT values were determined by subtracting the CT of the 16S rRNA housekeeping gene from the CT of the target gene, allowing for normalization of gene expression data. Comparative expression (ΔΔCT) was calculated as the difference between the ΔCT values of the test and reference strains. All statistical analyses were conducted using the R v4.4.1 software, and transcript changes were considered significant at $P < 0.05$.

2.10. Genomic and evolutionary analysis of gene sequences

The amino acid sequences of virulence-associated genes, including toxin-producing genes (*toxA–R*), lipase-encoding genes (*lipA/lipB*), pectinase-encoding genes (*pehA/pehB*), and genes responsible for chemotaxis and flagellar function (*che, flh, fli, tsr*, and *mot*), were selected for comparative genomic analysis. Virulence factor genes of the isolate *B. gladioli* BDBgla132A were compared using BLASTp against the BD_21g (*B. glumae)* proteome [29]. Also, virulence factor genes of the BDBgla132A and BD_21g isolates were compared against all publicly available *B. cepacia* proteomes using BLASTp. Percent identities were calculated as protein sequence identity.

To investigate the evolutionary history and distribution of virulence-related genes across the two *Burkholderia* species, the nucleotide sequences of virulence-linked genes, including toxoflavin biosynthesis genes (*toxA–R*), lipase-endocing genes (*lipA/lipB*), polygalacturonase-endoding genes (*pehA/pehB*), and chemotaxis/flagellar genes (*che, flh, fli, tsr, mot*) were retrieved from 28 bacterial strains representing the diversity of *B. glumae* and *B. gladioli*. These sequences were subsequently used to construct phylogenetic trees, enabling comparative analyses of virulence factor distribution and evolutionary divergence among isolates. The complete genome sequences for *B. glumae* strain BGR1 (GCF_000022645.2) and *B. gladioli* strains ABIP2048 (GCF_914484755.1), GSRB05 (GCF_019400155.1), UPMBG7 (GCF_027620325.1), UPMBG8 (GCF_027620475.1), BSR3 (GCF_000194745.1), KACC 18962 (GCF_036837415.1) and KACC 18963 (GCF_036839165.1) were retrieved from the GenBank database. Additionally, the genomes of *B. gladioli* and *B. glumae* strains BDBgla117A, BDBgla119A, BDBgla120A, BDBgla122A, BDBgla130A, BDBgla132A, BDBgla135A, BDBgla136A, BDBgla140A, BDBgla150A, BDBgla151A, BDBgla162A, BDBgla38A, BDBgla41A, BDBgla59A, BDBgla78A, BDBgla79A, BDBgla81A, BDBgla83A and BD_21g (*i.e.,* the 20 strains characterized in this study), were previously sequenced by us [29,30]. The MEGA software version 12 [44] was used to conduct phylogenetic analyses. For each gene cluster, nucleotide sequences were aligned using the ClustalW algorithm, as implemented in MEGA. Phylogenetic trees were constructed using the Maximum Likelihood method, and the Tamura–Nei model [45] of nucleotide substitutions was chosen by MEGA's model testing heuristic. The reliability of tree topologies was evaluated by conducting bootstrap analyses with 1,000 replicates, and clans with bootstrap values greater than 80% were considered reliable.

 doi:10.20944/preprints202601.1111.v2

3. Results

3.1. Isolation and Molecular Identification of Burkholderia Strains from Rice Panicles

A total of 300 bacterial isolates were obtained from the 300 BPB-infected rice panicle samples collected from 20 districts across Bangladesh during the 2022–2023 crop growing seasons [29,30]. The colony characteristics of these strains were compared with those of ATCC strains of several *Burkholderia* species. Most rice-infecting strains were similar in colony characteristics on S-PG medium, exhibiting circular, smooth, opalescent, and convex colonies with a purple center, as previously described [32]. The colonies were nonfluorescent under UV light and produced a yellow pigment on KBA. Bacterial colonies showing purple color on S-PG medium were selected and purified as candidate pathogens. Two types of colonies were observed: type A colonies (round colonies with smooth edges and reddish-brown discoloration), and type B colonies (round colonies with purple reflectors in the center of the magenta background (Figure 2A and 2B), as in ref. [46]. PCR assays targeting 16S rDNA and *gyrB* genes were used to detect *B. gladioli* and *B. glumae* in symptomatic rice panicles using species-specific primers, resulting in 479 bp (*B. gladioli*) and 529 bp (*B. glumae*) amplicons for *gyrB* (Figure 2C); and 1400 bp (*B. gladioli*) and 1494 bp (*B. glumae*) amplicons for 16S rDNA [29,30]. Out of the 300 isolates, 46 were preliminarily identified as *B. gladioli*, and 5 as *B. glumae* based on their characteristic colony morphology on S-PG medium, production of the yellow pigment toxoflavin on King's B agar, 16S rDNA and *gyrB* PCR amplification [29,30]. However, after sequencing the PCR products from both genes of the strains initially identified as *B. glumae*, only one was confirmed as *B. glumae*. Finally, one *B. glumae* and 19 *B. gladioli* isolates were selected for in-depth characterization based on successfully sequence and assemble their whole genomes, as described [29,30].

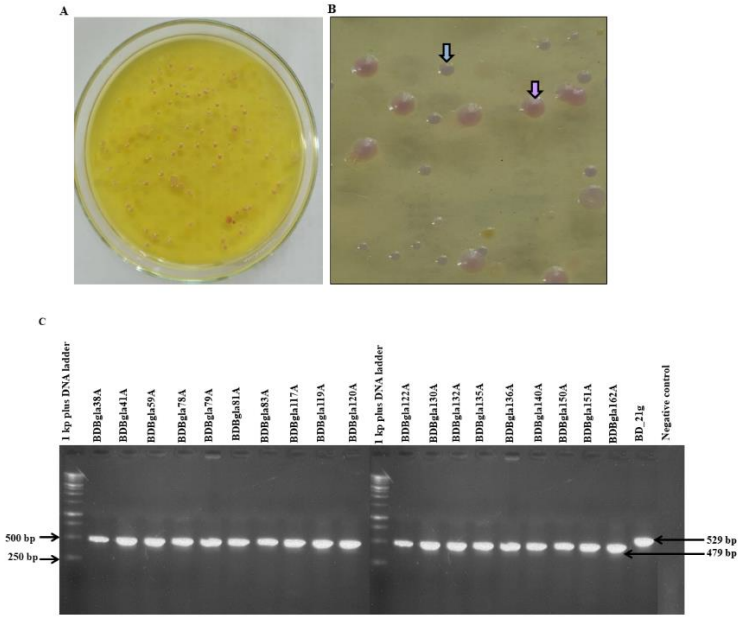

Figure 2. Morphological and molecular identification of target bacterial isolates. (A) Colonies on S-PG medium showing distinct morphology. (B) Enlarged views of selected colonies indicated by arrows: Type A colonies are round with smooth edges and reddish-brown discoloration, and Type B colonies are round with a central purple reflection on a magenta background. (C) Detection of BD_21g (*B. glumae*) and *B. gladioli* in infected rice panicles by PCR, with amplification of *gyrB* gene fragments of 479 bp and 529 bp, respectively except in the negative control (PCR reactions with no template DNA and sterile water).

3.2. Pathogenicity Assessment on Rice Plants

All 20 isolates tested exhibited pathogenicity on both rice panicles and seedlings. Of these, 17 isolates (85%) induced typical panicle blight symptoms and were classified as virulent, producing

 doi:10.20944/preprints202601.1111.v2

characteristic symptoms on both seedlings and panicles (Table 1). Notably, nine isolates (53%) caused severe disease symptoms, while eight (47%) induced moderate symptoms on both tissues. In contrast, three isolates (15%) produced only mild symptoms, limited to the panicles, and sterile water used as a negative control did not cause any symptoms (Figures 3A and 3B). Disease severity was assessed based on symptoms using a 0–9 rating scale, as described in ref. [33]. The symptoms induced by the two species were phenotypically indistinguishable. Koch's postulates were fulfilled by reisolating pathogens from representative infected samples.

Table 1. Pathogenicity test results of bacterial isolates from rice exhibiting bacterial panicle blight symptoms, and categorization based on isolate identity.

Isolate ID[a]	Species	Pathogenicity test[b]		Disease severity[c] (0-9 scale)
		Seedling	Panicle	
BD_21g	*B. glumae*	+++	+++	9.0 ± 0a***
BDBgla132A	*B. gladioli*	+++	+++	8.2 ± 0.23ab***
BDBgla117A	*B. gladioli*	+++	+++	7.8 ± 0.23ab***
BDBgla135A	*B. gladioli*	+++	+++	8.0 ± 0.31ab***
BDBgla122A	*B. gladioli*	+++	+++	7.9 ± 0.27ab***
BDBgla78A	*B. gladioli*	++	+++	7.2 ± 0.12ab***
BDBgla119A	*B. gladioli*	++	+++	7.3 ± 0.18b***
BDBgla136A	*B. gladioli*	++	+++	7.5 ± 0.58de***
BDBgla59A	*B. gladioli*	++	+++	7.0 ± 0.12bc***
BDBgla150A	*B. gladioli*	+	++	7.6 ± 0.31bc***
BDBgla81A	*B. gladioli*	+	++	5.7 ± 0.24bcd***
BDBgla120A	*B. gladioli*	+	++	5.9 ± 0.58cde***
BDBgla140A	*B. gladioli*	+	++	5.7 ± 0.29de***
BDBgla83A	*B. gladioli*	+	++	5.6 ± 0.31de***
BDBgla79A	*B. gladioli*	+	++	5.2 ± 0.12e***
BDBgla130A	*B. gladioli*	+	++	5.1 ± 1.16e***
BDBgla38A	*B. gladioli*	+	++	5.5 ± 0.35e***
BDBgla162A	*B. gladioli*	0	+	3.7 ± 0.29f***
BDBgla151A	*B. gladioli*	0	+	2.5 ± 0.73f***
BDBgla41A	*B. gladioli*	0	+	2.7 ± 0.87f***
Control	Sterile water	0	0	0.0 ± 0g

[a]Bacterial strains were isolated from panicle grains across Bangladesh. [b]Pathogenicity reactions were scored as +++ (highly virulent), ++ (moderately virulent), + (weakly virulent), and 0 (non-pathogenic). [c]Disease severity was scored on a 0–9 scale (0 = no symptoms; 1 = 0.1–10.0% of the panicle affected; 3 = 11–20% of the panicle affected; 5 = 21–30% of the panicle affected; 7 = 31–60% of the panicle affected; 9 = >61% of the panicle affected). Values are presented as means ± standard errors (SE) from three replicates (total $n = 63$). Differences among isolates were analyzed by a one-way ANOVA, followed by Duncan's multiple range test (DMRT) for mean separation when significant. Lowercase letters (a–g) indicate statistically significant differences among isolates ($P < 0.05$) according to DMRT; isolates sharing the same letter are not significantly different from each other. Asterisks indicate significance relative to the control (***, $P < 0.001$).

 doi:10.20944/preprints202601.1111.v2

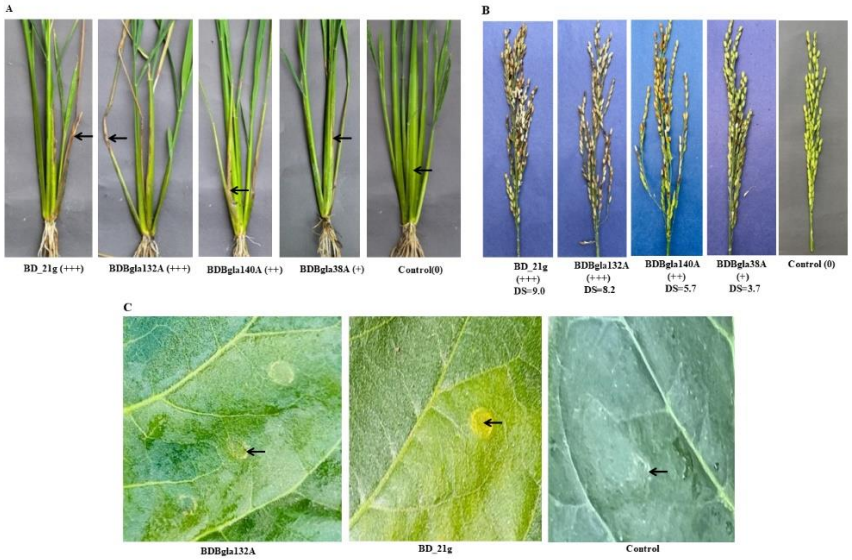

Figure 3. Assessment of pathogenicity and hypersensitive response assays. (A) Virulence evaluation of leaf sheath in rice seedlings (*Oryza sativa* L. cv. Horidhan) scored as + (weak), ++ (moderate), +++ (severe), or 0 (non-pathogenic) (B) Disease severity (DS) on rice panicles using a 0–9 scale. (C) Hypersensitive response in *Nicotiana tabacum* leaves 48 h after infiltration with ~10^8 CFU/mL of toxoflavin-producing strains; sterile water-infiltrated leaves showed no reaction. Arrows mark necrotic spots.

3.3. Onion Assays for Virulence Testing

The virulence of *Burkholderia* strains was evaluated by onion bulb scale assays. All virulent isolates of *B. glumae* and *B. gladioli* consistently caused significant maceration of onion bulb scales. The virulence potential of individual strains was determined by the ability to induce tissue maceration overlaying onion bulb scales. Bacterial suspensions with ~5 × 10^5 CFU/mL were inoculated and incubated at 30°C for 48 hours [34], revealing substantial variation in the macerated area among isolates (Figure 4A). The highly virulent strains BDBgla132A, BDBgla120A, BDBgla135A, BDBgla122A, BDBgla136A, and BD_21g showed extensive bulb maceration. Conversely, the strains BDBgla41A, BDBgla162A, BDBgla151A, BDBgla38A, and BDBgla83A exhibited considerably less tissue degradation. The negative control showed negligible maceration specificity to pathogen action (Figure 4B). The severity of maceration of onion bulbs showed a strong positive correlation with disease severity on rice panicles ($r = 0.83$, $P = 2.9 \times 10^{-6}$; Figure 4C), reinforcing the reliability of onion assays as a surrogate model for assessing rice pathogenicity.

 doi:10.20944/preprints202601.1111.v2

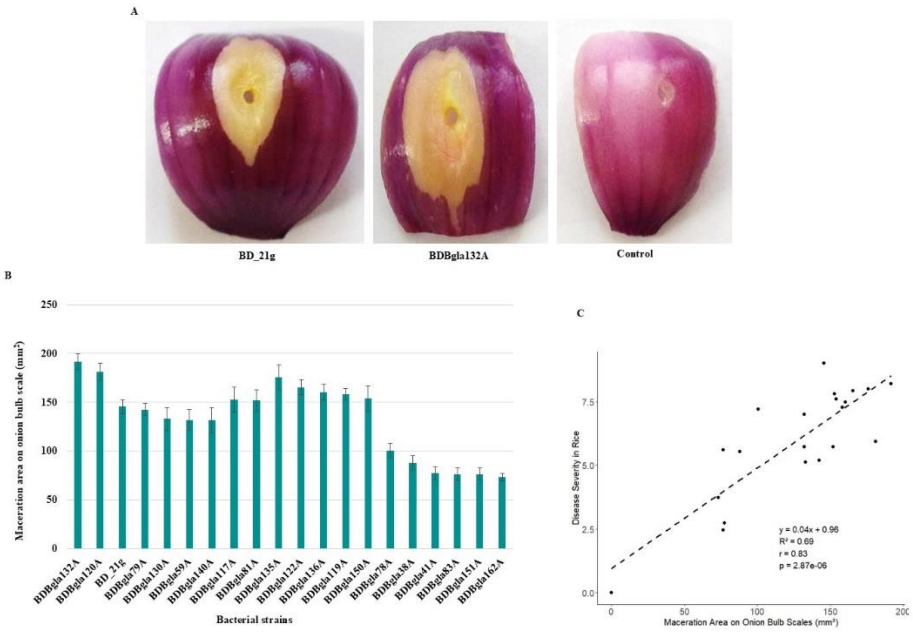

Figure 4. Virulence of *B. glumae* and *B. gladioli* strains on onion bulb scales and their correlation to rice panicle disease severity. (A) Onion bulb scales were inoculated with bacterial suspensions (~5 × 10^5 CFU/mL) and incubated at 30°C for 48 h post-inoculation; different isolates exhibited varying degrees of tissue maceration compared to sterile water (which was used as control). (B) The area of tissue maceration for each strain was measured. (C) Correlation between onion scale tissue maceration and rice panicle disease severity with a linear regression line. All regression coefficients were statistically significant ($P < 0.05$). Error bars represent standard errors from three biological replicates (total $n = 63$ scales). Differences among isolates in maceration area were analyzed by a one-way ANOVA, followed by DMRT for mean separation when significant ($P < 0.05$). Statistical analyses were performed in R version 4.4.1. .

3.4. Hypersensitive Response Elicitation

To evaluate the functionality of the Type III secretion system (T3SS) in *Burkholderia* strains, the capacity to elicit a hypersensitive response (HR) on *Nicotiana tabacum* leaves was tested. Bacterial suspensions (~5 × 10^7 CFU/mL) from toxoflavin-producing isolates were infiltrated into fully expanded tobacco leaves, and necrotic lesions, which are hallmarks of HR, were assessed at 24, 48, and 72 hours post-infiltration [35]. Lesions were visible in all isolates. By 48 h, strains BDBgla132A and BD_21g displayed unique lesion phenotypes (Figure 3C). Conversely, sterile water-infiltrated leaves did not exhibit a HR.

3.5. Toxoflavin Production and Quantification

Phenotypic characterization of the 20 bacterial isolates revealed that all strains produced toxoflavin, as evidenced by the appearance of bright yellow pigment on King's B (KB) agar plates following 48 hours of incubation at 37°C [8], while the negative control did not. However, the intensity of the pigment, which correlates with toxoflavin production levels, significantly varied among the strains. Importantly, the BD_21g (*B. glumae*) strain produced a brighter yellow pigment than the *B. gladioli* BDBgla132A strain–indicative of a higher production of toxoflavin by BD_21g (Figure 5A). Following bacterial cell removal, toxoflavin was extracted using chloroform (1:1 w/v) and visualized as a bright yellow solution (Figure 5B). The extracted toxoflavin was quantified using a spectrophotometer at 393 nm (Figure 5C). Quantitative results indicated strong toxoflavin production in all isolates, although the absorbance varied. The BD_21g strain produced the highest absorbance of toxoflavin, consistent with phenotypic observations, and the absorbance was significantly higher than that produced by BDBgla132A and other strains.

 doi:10.20944/preprints202601.1111.v2

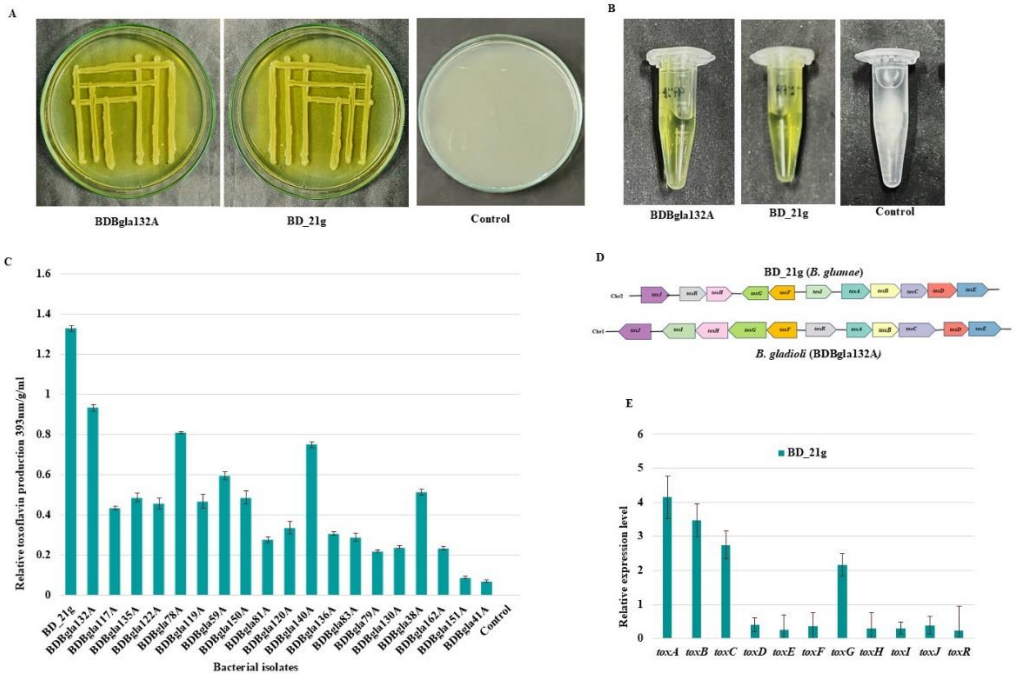

Figure 5. Toxoflavin production and molecular features of *B. glumae* and *B. gladioli* strains. (A) Toxoflavin phenotypes on King's B agar after incubation for 48 h at 37°C; all *Burkholderia* strains produced pigment while the negative control did not (B) Toxoflavin pigment extraction via chloroform following bacterial cell removal. (C) Spectrophotometric measurement of relative toxoflavin production at 393 nm. (D) Schematic representation of the toxin-producing gene clusters in two bacterial strains, BD_21g (*B. glumae*) and *B. gladioli* (BDBgla132A). In *B. glumae* (chromosome 2) the tox operon comprises the following genes in sequential order: *toxJ, toxR, toxH, toxG, toxF, toxI, toxA, toxB, toxC, toxD,* and *toxE*. In contrast, in *B. gladioli* (chromosome 1), the same genes are similarly arranged but with *toxR* relocated downstream of *toxF*. (E) Relative expression of the *toxA–toxR* genes was quantified by qPCR, normalizing to 16S rRNA and setting *B. gladioli* (BDBgla132A) expression to 1 for the control strain, whereas *B. glumae* (BD_21g) served as the test strain. Error bars represent standard errors from three independent biological replicates. All differences between groups were evaluated in R (version 4.4.1) using an ANOVA with Duncan's multiple range test (DMRT) for multiple comparisons ($n = 63$) and Student's *t*-tests for pairwise comparisons ($n = 33$), with statistical significance set at $P < 0.05$.

3.6. Lipase Activity Assessment and Quantification

Lipase activity in *Burkholderia* strains was determined by combining phenotypic screening with quantitative enzyme assays. The qualitative plate assays on LB agar supplemented with 5% Tween 20 revealed high levels of lipase activity, as evidenced by opaque halos formed around the isolates [37], which were not present in the negative control. While all tested isolates produced lipase, the most virulent strains, BD_21g and BDBgla132A, exhibited distinctly prominent opaque halos, indicating robust extracellular lipase secretion and confirming the specificity of the lipase-induced phenotype (Figure 6A). A chromogenic substrate assay using p-nitrophenyl palmitate confirmed lipase production in all strains, as evidenced by the distinct yellow color resulting from p-nitrophenol release, whereas the control showed no color change (Figure 6B). Quantitative spectrophotometric measurement at 410 nm demonstrated that BD_21g isolates displayed the highest lipase activity, followed by BDBgla132A, while the other isolates exhibited significantly lower activity (Figure 6C). No lipase activity was detected in the control.

 doi:10.20944/preprints202601.1111.v2

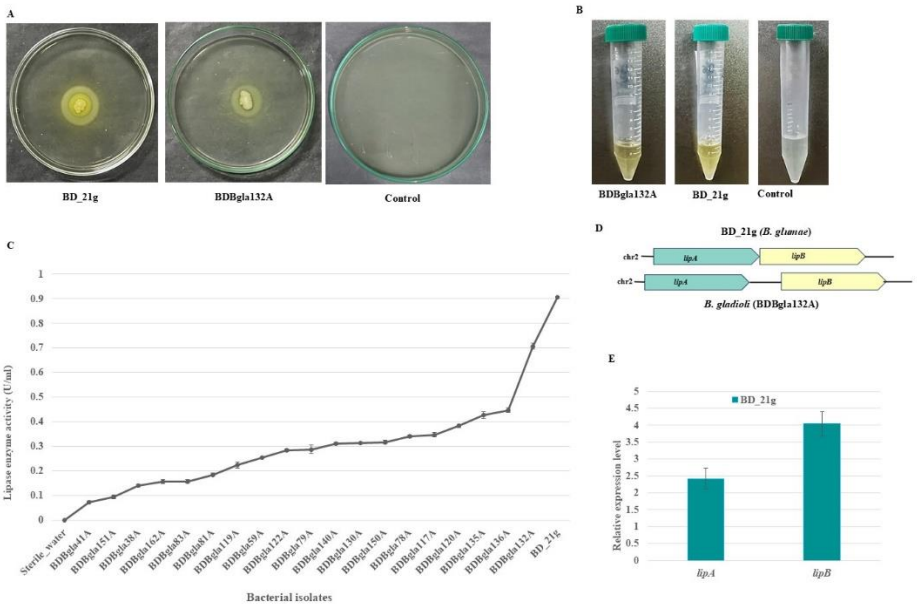

Figure 6. Phenotypic traits of lipase production in BD_21g (*B. glumae*) and *B. gladioli*. (A) Extracellular lipase activity on LB agar supplemented with 5% Tween 20, indicated by opaque halos surrounding BD_21g and BDBgla132A colonies; the negative control showed no activity. (B) Chromogenic assay with p-nitrophenyl palmitate, indicating lipase activity by yellow coloration in the test strains but not in the control. (C) Spectrophotometric measurement of lipase activity across multiple bacterial isolates at 410 nm. (D) Comparative genomic organization of the lipase-encoding genes *lipA* (teal) and *lipB* (yellow) in BD_21g (*B. glumae*) and *B. gladioli* (strain BDBgla132A). Both species exhibit tandem co-localization of *lipA* and *lipB* on chromosome 2 in the same orientation (*lipA* upstream of *lipB*), differing only in intergenic spacing. (E) Relative expression of *lipA* and *lipB* transcripts in BD_21g (*B. glumae*) compared to *B. gladioli* BDBgla132A (set to 1). Error bars denote standard errors calculated from three independent biological replicates. All observed differences between groups were analyzed in R (version 4.4.1) using a one-way ANOVA followed by Duncan's multiple range test ($n = 63$) for multiple comparisons and Student's *t*-tests ($n = 6$) for pairwise comparisons, with significance defined as $P < 0.05$.

3.7. Qualitative and Quantitative Evaluation of Polygalacturonase Activity

The activity of polygalacturonase (PG) in *Burkholderia* isolates was investigated through a combination of phenotypic and quantitative enzyme assays. Isolates were grown on semi-solid pectate-yeast agar (PEC-YA) media for phenotypic expression [39]. Each strain induced clear halo zones around the colonies, indicating significant pectinolytic activity consistent with polygalacturonate degradation. This was particularly evident in the *B. gladioli* isolate BDBgla132A and the BD_21g (*B. glumae*) (Figure 7A). No halos were observed in the control. Next, all 20 isolates were cultured in M9 minimal medium [40] supplemented with polygalacturonic acid to induce polygalacturonase expression. Culture supernatants were collected after 48 h of incubation at 30°C and assayed for enzymatic activity using a modified Bernfeld method [41]. This colorimetric assay was applied to measure the amount of galacturonic acid released from PGA by spectrophotometry at 530 nm. All isolates exhibited readily detectable polygalacturonase activity when grown in PGA-supplemented medium, whereas none of them exhibited detectable activity in the control medium lacking the substrate (Figure 7B). Among the tested strains, *B. gladioli* BDBgla132A and BDBgla136A consistently exhibited the highest enzymatic activities (Figure 7C). Interestingly, most of the *B. gladioli* isolates showed higher polygalacturonase activity than the BD_21g (*B. glumae*), which may contribute to their increased virulence and ability to degrade plant cell walls more effectively.

 doi:10.20944/preprints202601.1111.v2

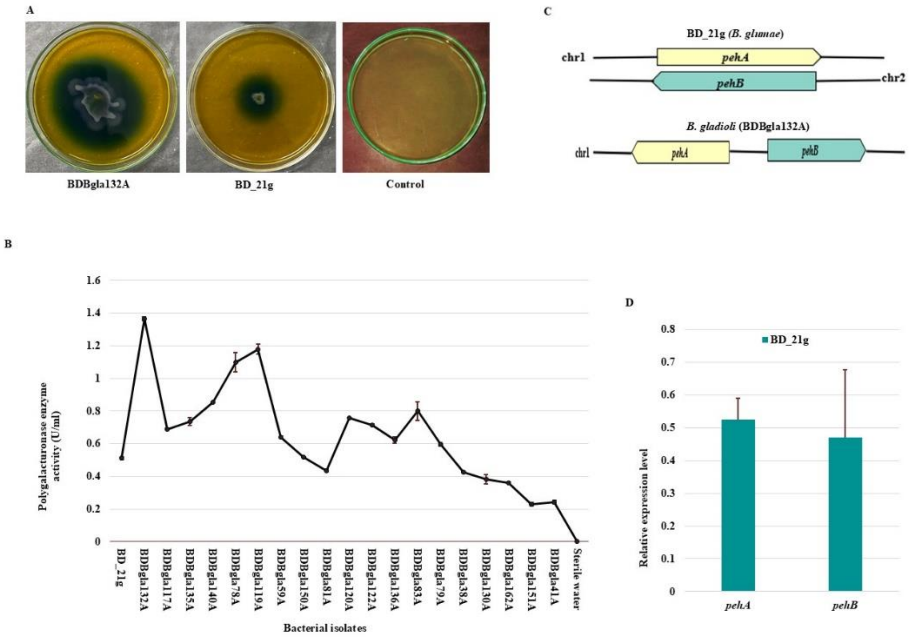

Figure 7. Phenotypic and molecular characterization of polygalacturonase activity in BD_21g (*B. glumae*) and *B. gladioli*. (A) Pectinolytic activity on semi-solid pectate-yeast agar (PEC-YA) showing halo formation around BDBgla132A and BD_21g colonies, unlike the negative control (B) Quantitative spectrophotometric measurement of polygalacturonase activity at 530 nm. (C) Comparative genomic organization of polygalacturonase-encoding genes *pehA* (yellow) and *pehB* (teal) in BD_21g (*B. glumae*) and BDBgla132A (*B. gladioli*). In BD_21g (*B. glumae*), *pehA* and *pehB* are located on separate replicons (chromosomes 1 and 2, respectively), whereas in *B. gladioli* both genes are arranged in tandem on chromosome 1. (D) Relative expression levels of *pehA* and *pehB* in BD_21g compared to BDBgla132A (expression normalized to 1). Statistical analyses were performed in R (v4.4.1). A one-way ANOVA with DMRT (n = 63) assessed group differences, while Student's t-tests (n = 6) evaluated pairwise comparisons. Significance was set at $P < 0.05$.

3.8. Swarming Motility Assessment

The rapid motility of BD_21g (*B. glumae*) and *B. gladioli* isolates was analyzed. Swarming motility assays (Figure 8A) showed dendritic bacterial spreading patterns, with BDBgla132A exhibiting the best motility, followed by BD_21g. Sterile standard LB agar (1.5% agar) without the low-agar modification served as the negative control and showed no spreading, confirming that the reduced agar concentration was essential for swarming motility. The diameter of the motility zones was determined, and *B. gladioli* isolate BDBgla132A exhibited the largest motility zone diameter, followed by strains BDBgla136A, BDBgla162A, BDBgla83A, BDBgla81A, and BD_21g (Figure 8B).

 doi:10.20944/preprints202601.1111.v2

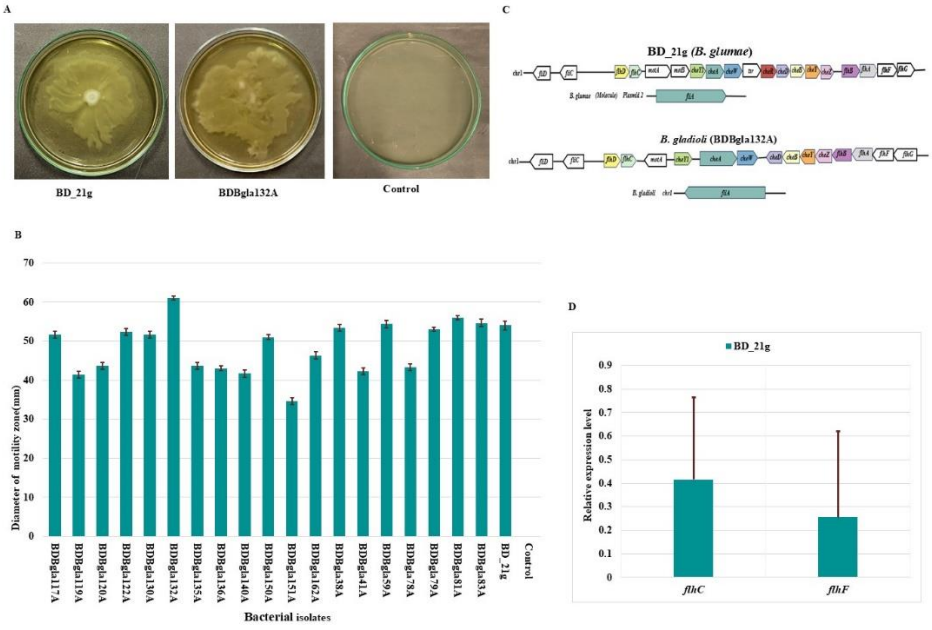

Figure 8. Phenotypic and molecular features of motility in BD_21g (*B. glumae*) and *B. gladioli*. (A) Swarming motility assays on 0.5% LB agar, showing the characteristic dendritic spreading for the positive isolates but not for the negative control (B) Quantitative measurement of swarming motility across *Burkholderia* strains, expressed as the diameter of motility zone on agar plates incubated at 34 °C. (C) Genomic organization of motility and chemotaxis gene clusters in BD_21g (*B. glumae*) and *B. gladioli*. Chromosomal loci (chromosome 1) from BD_21g (*B. glumae*) and *B. gladioli* BDBgla132A (top and middle) show adjacent genes including *fliD, fliC, flhD, flhC, motA, cheY, cheA, cheW, cheD, cheB, cheZ, flhB, flhA, flhF,* and *flhG*. The *B. glumae* plasmid 2 and *B. gladioli* chromosome 1 fragments (second and bottom) each contain the *fliA* gene. Color coding highlights conserved homologous genes between strains. (D) Relative expression of flagellar regulatory genes *flhF* and *flhC* in BD_21g (*B. glumae*) normalized to expression in *B. gladioli* strain BDBgla132A (set to 1). Error bars represent standard errors from three biological replicates. Statistical analyses were performed using R v4.4.1. All statistical analyses were conducted in R (v4.4.1). Group means were compared using a one-way ANOVA with Duncan's multiple range test (DMRT; $n = 63$), while pairwise comparisons were evaluated with Student's *t*-tests ($n = 6$). Statistical significance was established at $P < 0.05$.

3.9. Differential Expression of Virulence-Associated Genes

Quantitative reverse transcription PCR quantifies expression fold-changes to identify genes operationally engaged during infection, differentiating between genetic capacity for pathogenesis and actively deployed virulence mechanisms. This approach elucidates the regulatory distinctions underlying divergent pathogenic strategies. Gene expression levels were quantified using the ΔΔCt method with real-time quantitative PCR (qPCR), normalized against the constitutive housekeeping gene 16S rRNA. Three biological replicates were performed for each of the two most virulent strains, with *B. gladioli* BDBgla132A serving as the reference (calibrator) and BD_21g (*B. glumae*) as the test strain. BD_21g exhibited significantly higher expression of key tox genes compared to BDBgla132A (Figure 5E). Specifically, *toxA* expression increased 4.15-fold, while *toxB, toxC,* and *toxG* showed increases of 3.5-fold, 2.8-fold, and 2-fold, respectively. The toxin gene expression pattern observed in BD_21g, which is consistent with its increased toxoflavin production, supports its association with increased virulence. However, *toxD, toxE, toxF, toxH, toxJ,* and *toxR* showed minimal expression differences between the two isolates, indicating a limited contribution to strain-specific differences in virulence. The expression levels of lipase-encoding genes *lipA* and *lipB* were 2.4- and 4-fold higher in BD_21g than in BDBgla132A (Figure 6E), respectively, which correlates with BD_21g's higher lipolytic activity. However, BD_21g showed 1.9-fold and 2-fold lower *pehA* and *pehB* transcript levels, respectively, than BDBgla132A (Figure 7D), suggesting other mechanisms of differential regulation

 doi:10.20944/preprints202601.1111.v2

of polygalacturonase-encoding genes. The same pattern was observed for flagellar regulatory genes: the expression levels of *flhC* and *flhF* were 2.4- and 3.8-fold lower for BD_21g than for BDBgla132A, respectively (Figure 8D). The observed differences in expression patterns suggest that BDBgla132A relies primarily on pectinolytic enzymes and motility for virulence, while BD_21g employs lipase and toxoflavin as its main virulence determinants.

3.10. Comparative Genomic and Evolutionary Analysis of Virulence-Associated Gene Clusters

Table 2 presents a comparative genomic analysis of virulence-associated genes between *B. gladioli* BDBgla132A and BD_21g (*B. glumae*) based on amino acid sequence identity. This analysis encompasses 35 virulence genes associated with five major virulence factors: toxoflavin, lipase, polygalacturonase, flagella, and chemotaxis regulators. The comparison uncovers considerable sequence identity and shared virulence factors between the two isolates. Genomic comparison of tox operons elucidates whether both species have retained genes required for toxoflavin production and establishes the level of sequence identity or variation present in these pathogenic determinants. Toxoflavin operons demonstrated high sequence identity between the two species. Toxoflavin biosynthesis-related genes (*toxABCDE*) exhibited the highest identity between the two strains, with *toxB* showing the highest identity at 98.11% followed by *toxC* at 97.51%. Transport-related genes (*toxFGHI*) maintained high sequence identity, particularly *toxH* at 97.48%. However, *toxI* exhibited substantially lower identity at 44.35%, indicating significant genetic divergence in this gene between the two strains. CDD analysis classified *toxI* from both BDBgla132A (WP_439967532.1) and BD_21g (WP_230674341.1) as members of the PRK09837 Cu(I)/Ag(I) efflux RND transporter outer membrane protein family, with additional hits to TolC, outer_NodT, and OEP outer membrane factors spanning nearly the entire sequence length. Despite 44.35% amino acid identity, both *toxI* homologs share the same TolC-like outer membrane channel architecture, confirming the conservation of efflux function across strains. Transcriptional regulators showed variable identity: *toxJ* demonstrated moderate identity at 77.5%, while *toxR* retained high identity at 96.01%. Sequence identity analysis of virulence determinants (*lipA*/*lipB*, *pehA*/*pehB*, and motility genes) revealed patterns of conservation and divergence across species. Sequence identity analysis of the lipase gene family revealed differential similarity between the two species: *lipA* showed substantial identity (88.55%), while *lipB* exhibited lower identity (80.71%). Polygalacturonase-encoding genes (*pehA* and *pehB*) maintained moderate-to-high identity, with *pehA* at 84.53% and *pehB* at 87.35%. The core chemotaxis-related genes (*cheA*, *cheB*, *cheD*, *cheW*, *cheY*, *cheY1*, *cheZ*) maintained high identity (80.80–97.22%). Notably, *cheR* was present in BD_21g (*B. glumae*) but absent in *B. gladioli* BDBgla132. This lineage-specific absence may reflect divergent chemotaxis regulation mechanisms between the two species. The flagellum-related biosynthesis genes (*flhA*–*fliD*) showed highly variable identity, ranging from 66.92% to 96.72% Among these, *flhC* showed the highest identity at 96.72%, while *fliD* displayed substantially lower identity at 66.92%. The *motA* gene retained strong sequence identity at 96.5% reflecting its importance in driving flagellar rotation via a chemiosmotic gradient. Conversely, *motB* and *tsr*, which encode a component of the flagellar motor and a chemotactic receptor, respectively, were present in BD_21g (*B. glumae*) but absent in *B. gladioli* BDBgla132A, suggesting species-specific retention of flagellar genes.

Table 2. Homology of virulence-associated genes between the BDBgla132A (*B. gladioli*) and BD_21g (*B. glumae*) genomes.

Virulence factor	Gene	Gene accession (BDBgla132A)	Gene accession (BD_21g)	Protein identity (%)
Toxoflavin	*toxA*	WP_047837656.1	WP_230674340.1	96.23
	toxB	WP_013696509.1	WP_042967738.1	98.11
	toxC	WP_186032113.1	WP_012733473.1	97.51
	toxD	WP_186146217.1	WP_012733474.1	96.63

 doi:10.20944/preprints202601.1111.v2

	toxE	WP_186044336.1	WP_017922993.1	71.07
	toxF	WP_186146218.1	WP_012733469.1	92.67
	toxG	WP_186012765.1	WP_012733468.1	92.08
	toxH	WP_439968039.1	WP_251107611.1	97.48
	toxI	WP_439967532.1	WP_230674341.1	44.35
	toxJ	WP_047838500.1	WP_012733464.1	77.50
	toxR	WP_047837657.1	WP_012733470.1	96.01
Lipase	*lipA*	WP_047838330.1	WP_012733585.1	88.55
	lipB	WP_440015440.1	WP_251107590.1	80.71
Polygalacturonase	*pehA*	WP_186012903.1	WP_017922174.1	84.53
	pehB	WP_439967530.1	WP_017423921.1	87.35
Chemotaxis and flagella	*cheA*	WP_440017944.1	WP_251107216.1	97.22
	cheB	WP_047836241.1	WP_012734288.1	96.06
	cheD	WP_036029515.1	WP_012734287.1	93.07
	cheR	Absent	-	-
	cheW	WP_043219446.1	WP_012734284.1	92.57
	cheY	WP_013696282.1	WP_012734289.1	96.18
	cheY1	WP_013696275.1	WP_302074279.1	80.80
	cheZ	WP_047836242.1	WP_012734290.1	84.52
	flhA	WP_036038249.1	WP_012734295.1	95.86
	flhB	WP_013696287.1	WP_100556214.1	89.72
	flhC	WP_013696272.1	WP_012734279.1	96.72
	flhD	WP_025099997.1	WP_043226645.1	96.23
	flhF	WP_440017650.1	WP_251107218.1	93.19
	flhG	WP_013696290.1	WP_012734297.1	84.39
	fliA	WP_013696291.1	WP_017433111.1	95.67
	fliC	WP_186011140.1	WP_100556208.1	90.10
	fliD	WP_047836234.1	WP_012734272.1	66.92
	motA	WP_013696273.1	WP_012734280.1	96.50
	motB	Absent	-	-
	tsr	Absent	-	-

When compared with *B. cepacia*, the virulence-related proteins of both strains showed significant amino acid identity yet important differences in their virulence genes (Table S3), revealing differential pathogenic potential and evolutionary insights. The toxoflavin biosynthetic operons exhibited strong sequence identity across all three species, with core biosynthetic genes (*toxABCDE*) sharing 73.76–95.55% amino acid identity with *B. cepacia*, especially *toxB* (93.33–94.44%) and *toxC* (95.20–95.55%), while transport genes (*toxF*, *toxG*) showed markedly lower identity (57.14–73.62%). However, BD_21g exhibits marginally higher identity in *toxI* (88.8% vs. 62.56%) and *toxH* (95.91% vs. 78.58%), suggesting an enhanced toxin production potential. Lipase-encoding genes (*lipA*/*lipB*) are similarly conserved with moderate to high identity (59–80%), maintaining comparable nutrient acquisition capabilities. Both strains retain a *pehA* gene with high identity (83–94%), indicating capacity for plant cell wall degradation, yet both completely lack *pehB*, reflecting parallel loss of this supplementary pectin-degrading enzyme relative to *B. cepacia*. Chemotaxis and flagellar gene families exhibited the most complex evolutionary patterns. Core chemotaxis proteins (*cheA*, *cheB*, *cheD*, *cheW*, *cheY*, *cheZ*) shared high identity (82.06–100%) with their *B. cepacia* homologs, with *cheY* and *cheZ* showing perfect

 doi:10.20944/preprints202601.1111.v2

identity (100%) in BDBgla132A. Notably, *cheY1* exhibited substantially reduced identity (67.50–68.29%), indicating divergent selection in this chemotaxis-related protein. BD_21g possesses a *cheR* gene (81.85% identity), while the gene is completely absent from BDBgla132A. Flagellar biosynthesis genes varied substantially in their levels of conservation: *flhC* maintained particularly high identity (92.4–97.33%), *flhF* showed intermediate identity (69.79–83.5%), and *flhD* and *fliD* displayed markedly reduced identity (56.92–62.86%). Motor-encoding genes also varied in their levels of conservation, with *motA* showing high identity (93.36–94.41%), but with *motB* being absent in BDBgla132A, yet present in BD_21g (84.39%). Similarly, the chemotactic receptor *tsr* was absent in BDBgla132A but present in BD_21g (70.15%). The results indicate that both strains share a common ancestral virulence scaffold relative to *B. cepacia* but followed somewhat divergent evolutionary paths: BDBgla132A selectively lost chemotactic sensing genes (*cheR*, *tsr*) and flagellar motor function genes (*motB*), whereas BD_21g retained the ancestral motile, chemotactically-responsive strategy. These patterns suggest that both rice panicle blight pathogens specialized from an ancestral *Burkholderia* lineage through selective retention or loss of virulence-associated genes while maintaining core pathogenic functions.

Phylogenetic analyses of the four systems (toxoflavin, lipase, polygalacturonase, and flagellum-related genes) were conducted in MEGA 12 [44] using the Maximum Likelihood method [45] with 1,000 bootstrap replicates. For each system, concatenated nucleotide alignments of the respective gene sets from 26 *B. gladioli* and 2 *B. glumae* strains were used to construct the trees. Phylogenetic trees (Figures 9–12) show that the 11 tox-operon genes, two lipase genes, two polygalacturonase genes, and 20 flagellar genes from each isolate cluster closely with homologs from other strains, indicating no significant divergence among the examined strains. This clustering pattern suggests that these virulence factors have been conserved across the *B. gladioli* and *B. glumae* strains examined.

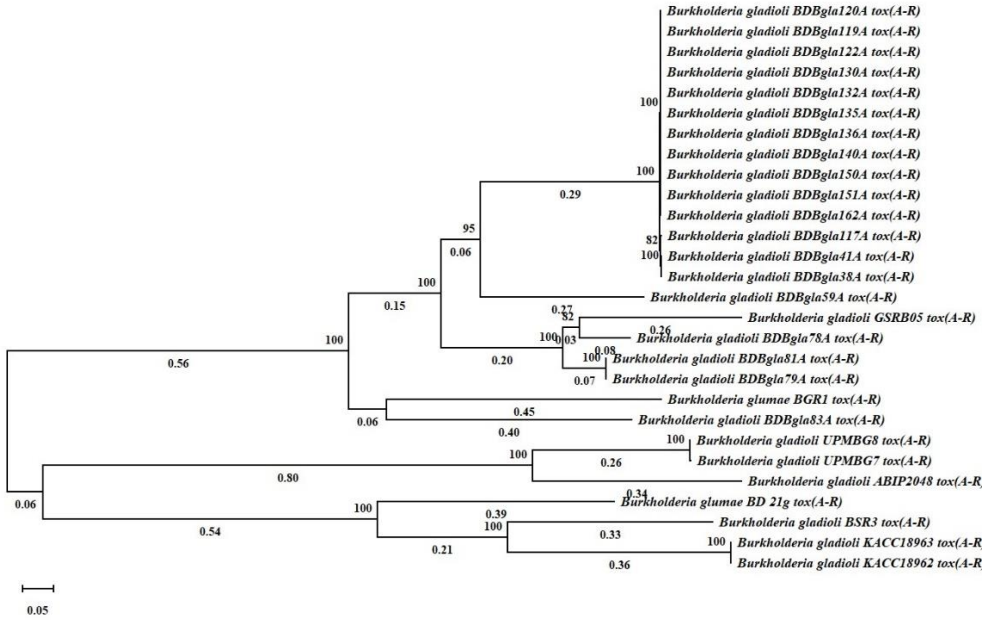

Figure 9. Phylogenetic tree of concatenated toxoflavin synthesis genes (*toxA, toxB, toxC, toxD, toxE, toxF, toxG, toxH, toxI, toxJ,* and t*oxR*) from *B. gladioli and B. glumae*. The tree was constructed using the Maximum Likelihood method with the Tamura–Nei [45] substitution model in MEGA 12 software [44], based on concatenated alignment of 28 nucleotide sequences (21,891 bp total). Bootstrap support values (1,000 replicates, ≥80% threshold) are shown at branch nodes. Branch lengths represent nucleotide substitutions per site.

 doi:10.20944/preprints202601.1111.v2

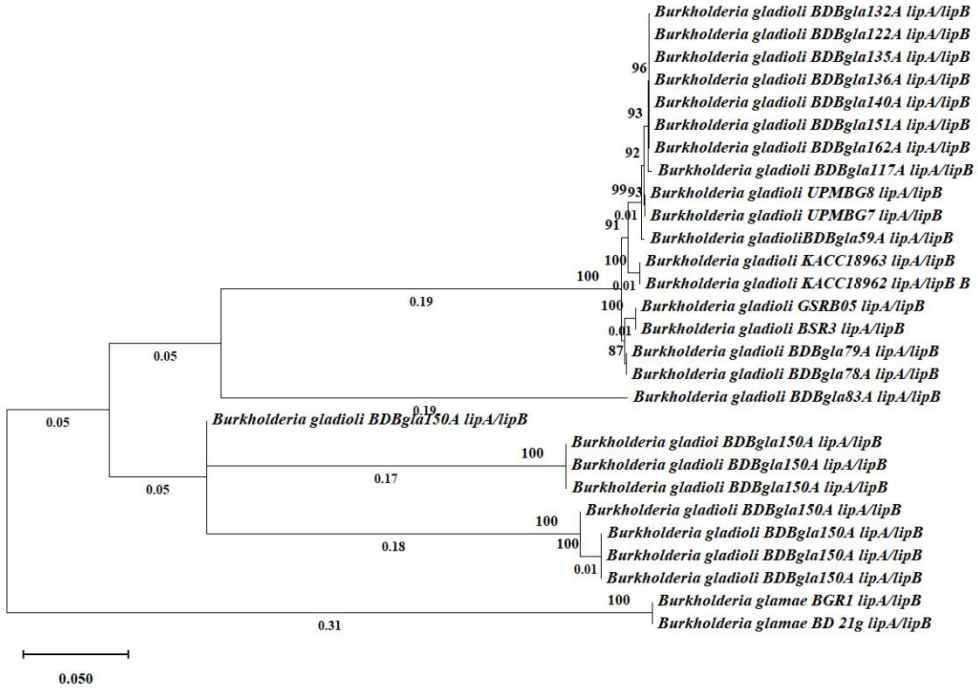

Figure 10. Phylogenomic analysis of concatenated lipase-encoding genes (*lipA/lipB)* from *B. gladioli and B. glumae*. The tree was constructed using the Maximum Likelihood method with the Tamura–Nei [45] substitution model in the MEGA 12 software [44], based on concatenated alignment of 28 nucleotide sequences (2,136 bp). Bootstrap support values (based on 1,000 replicates) are shown at branch nodes. Branch lengths represent nucleotide substitutions per site.

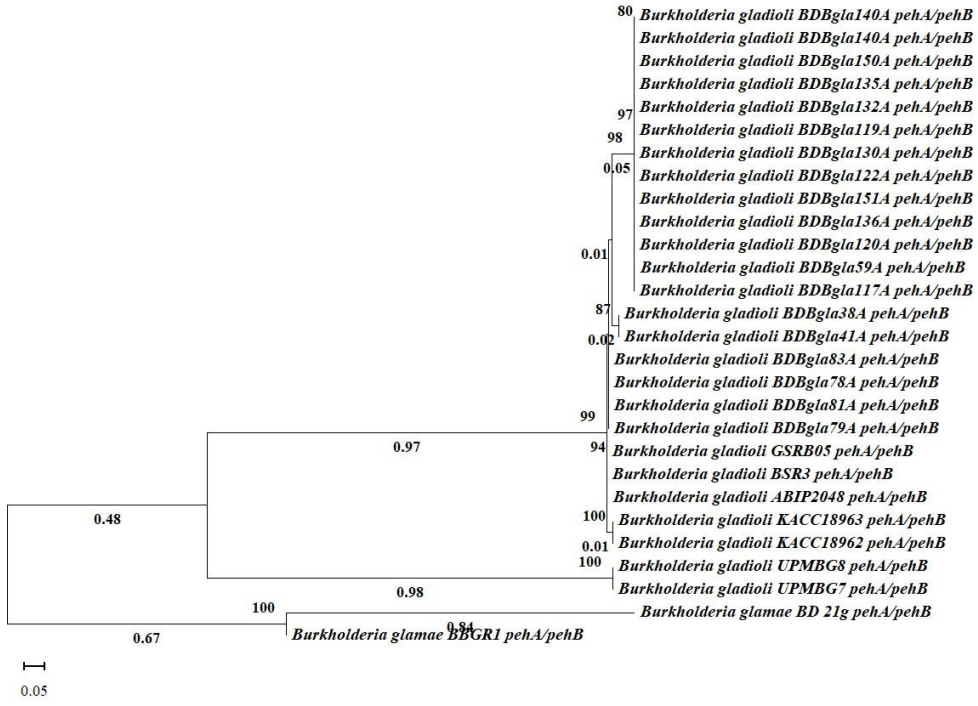

 doi:10.20944/preprints202601.1111.v2

Figure 11. Molecular phylogeny of pectinase-encoding genes of concatenated pectinase-encoding genes (*pehA*/*pehB*) from *B. gladioli and B. glumae*. Maximum Likelihood phylogeny (Tamura–Nei model [45]) was inferred in MEGA 12 [44] from 28 concatenated nucleotide sequences (4,488 bp). Bootstrap support values (1,000 replicates) are indicated at nodes; branch lengths represent nucleotide substitutions per site.

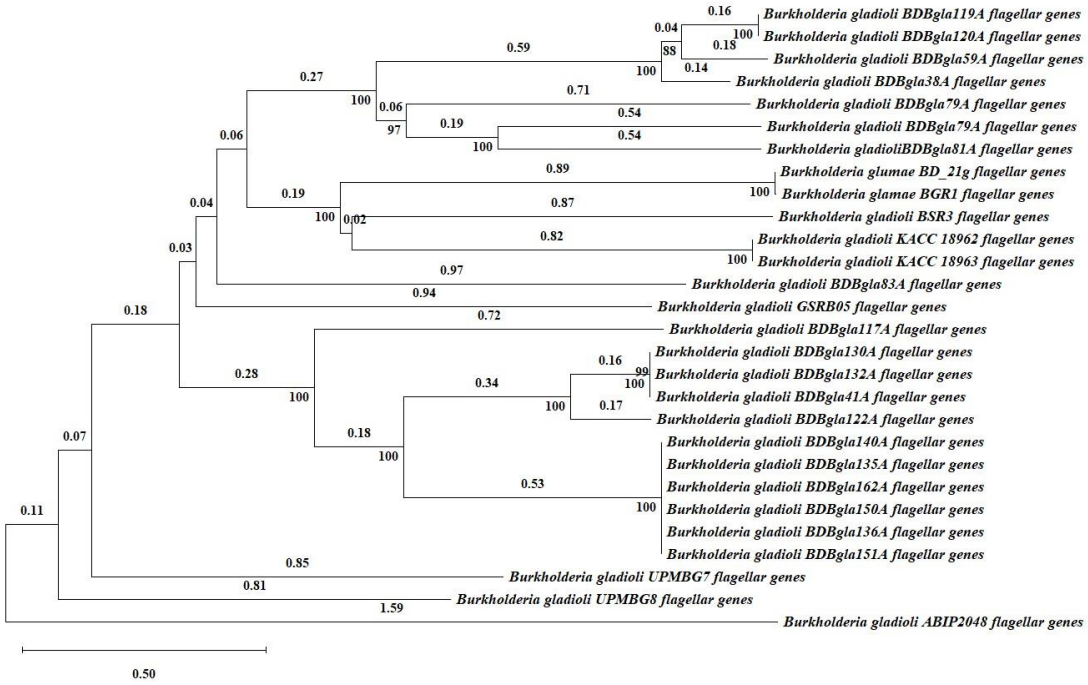

Figure 12. Maximum Likelihood phylogeny of concatenated flagellum-encoding genes (*cheA, cheB, cheD, cheR, cheW, cheY, cheY1, cheZ, flhA, flhB, flhC, flhD, flhF, flhG, fliA, fliC, fliD, tsr, motA, and motB*) from *B. gladioli* and *B. glumae*. The tree was constructed using the Tamura–Nei [45] substitution model in MEGA 12 software [44] based on 19 concatenated genes from 28 nucleotide sequences (24,645 bp). Bootstrap support values (1,000 replicates) are shown at branch nodes. Branch lengths represent nucleotide substitutions per site. Branches with <80% bootstrap support were collapsed.

4. Discussion

A comprehensive investigation of *Burkholderia* species in association with bacterial panicle blight (BPB) of rice in Bangladesh is presented. A total of 51 bacterial strains were isolated from eight rice varieties collected across 20 districts during the 2022–2023 cropping season. S-PG and KBA media were suitable for preliminary screening, based on colony morphology and pigment formation, as described [8]. Two distinct colony types were observed: Type A, which formed reddish-brown colonies, and Type B, which showed a purple hue. These characteristics were consistent with those previously described [46], reinforcing the importance of these morphological traits in the early stages of identification. Further molecular identification using the PCR designed to amplify the *gyrB* gene [9] enabled accurate species determination, producing amplicons of 479 and 529 bp for *B. gladioli* and *B. glumae*, respectively. For species identification (*gyrB* PCR), this assay distinguishes *B. glumae* from *B. gladioli* based on conserved gene sequences, enabling accurate species confirmation beyond phenotypic traits. PCR-based methods are standard tools for distinguishing closely related bacterial pathogens, and newer real-time formats such as qPCR and RT-qPCR offer greatly improved sensitivity and quantitative capability for detection and gene expression analysis [9,12]. PCR-based detection of species revealed a marked predominance of *B. gladioli* (46/51) isolates with only 5 *B. glumae*. This dominance of *B. gladioli* is in accord with recent patterns found across South and Southeast Asia, where *B. gladioli* is becoming the most common BPB-causing pathogen, in contrast

 doi:10.20944/preprints202601.1111.v2

with previous reports in Japan and the America, where *B. glumae* was the primary causative agent [2,3]. *B. gladioli* were also detected in asymptomatic rice seeds in China in 2007, and the isolated strain induced disease symptoms when inoculated onto rice plants [47]. The relatively low occurrence of *B. glumae* in the survey may reflect differences in temperature and humidity regimes, cropping seasons, and local rice genotypes in Bangladesh, which together could favor *B. gladioli* over *B. glumae*. Overall, the evidence presented here supports the emerging importance of *B. gladioli* as a significant component of the BPB disease complex and highlights the need for reassessing the prevalence of the pathogen in other rice-growing endemic areas.

Toxoflavin biosynthesis in *Burkholderia glumae* reaches peak levels at 37°C [17]. In Bangladesh's rice-growing regions, mean daily maximum temperatures during the bacterial panicle blight (BPB) development season (March–November) typically range from 32 to 35°C, with frequent excursions above 37°C. To simulate these field conditions and to achieve optimum toxoflavin production, all pathogenicity tests in this study were conducted under controlled temperature regimes equivalent to diurnal temperatures ranging from 37 to 41°C. This temperature range maximizes toxoflavin synthesis while remaining physiologically related to the thermal environment of BPB development in Bangladesh. Pathogenicity tests confirmed that all studied *Burkholderia* strains produced BPB symptoms in both rice seedlings and panicles and that *the B. glumae* isolate was more virulent than the *B. gladioli* strains on both rice tissues. These findings are consistent with previous studies from Japan and Taiwan, which have found that rice plants grown in kernels at the boot or heading stages are more susceptible than seedlings at the four-leaf stage [48,49]. Onion assay tests demonstrated that all virulent isolates caused substantial tissue maceration with their ability to cause onion maceration being highly correlated with rice panicle disease severity suggesting the surrogate value of the assay for rice pathogenicity. This result is in agreement with those of previous studies on *Burkholderia cepacia* complex members, such as *B. cepacia* and *B. cenocepacia,* which cause soft rot symptoms in onion bulbs [50,51]. Similarly, Karki *et al*. [52] found a strong correlation between the virulence of *B. glumae* on onion bulbs and its virulence on rice panicles, supporting the importance of this assay for strain pathotyping. Given its simplicity, ease of replication, and potential expandability, the onion bulb scale assay has emerged as a novel method for *Burkholderia* pathogenicity testing.

B. glumae synthesizes two main isomeric toxins, namely toxoflavin and fervenulin [15]. As a phytopathogen, *B. glumae* secretes toxoflavin, which impedes the development of rice seedlings and affects the growth of both roots and shoots. Moreover, in the grain-rot phase, it contributes to the emergence of chlorosis primarily on the panicles [53,54]. The production of toxoflavin is significantly temperature-dependent, beginning at 30°C and reaching its maximum at 37°C [17]. The inability of certain *B. glumae* strains to produce toxoflavin prevents them from causing chlorosis, demonstrating the toxin's critical role in symptom development [16]. Phenotypic investigation of 20 isolates showed significant inter-strain variation in toxoflavin production, pigment patterns, and toxin quantification among the virulent isolates tested. This discrepancy could stem from differences in susceptibility to environmental signals among biosynthetic complexes, or from substantial differential regulation of quorum-sensing circuits such as TofR and TofI [22]. The distinction in virulence strategies between the BD_21g (*B. glumae*) and BDBgla132A (*B. gladioli*) strains is further highlighted by comparative gene expression. In BD_21g, toxoflavin biosynthesis genes exhibit higher levels of expression than in BDBgla132A. Among these, *toxA* exhibited the highest overall overexpression (4.15-fold), suggesting that a ToxA-type virulence strategy is present in that strain. In *B. glumae*, the *toxABCDE* operon encodes the enzymatic machinery for toxoflavin biosynthesis, while the *toxFGHI* operon encodes transporters that facilitate toxoflavin secretion [15,53,54]. *Quorum sensing* regulates toxoflavin production in *B. glumae* through N-octanoyl homoserine lactone, which is synthesized by the TofI enzyme and recognized by the TofR receptor C8-HSL. TofR activation leads to the expression of the toxoflavin production-associated transcriptional regulators ToxJ and ToxR [23]. *Notably, minimal differences in the expression of toxJ and toxR among strains, despite high toxA expression in BD_21g, suggest that this strain may employ non-canonical regulatory mechanisms beyond the classical TofI/TofR quorum-sensing pathway. A recent study has revealed that B. glumae possesses multiple alternative regulatory circuits*

 doi:10.20944/preprints202601.1111.v2

for toxoflavin biosynthesis, including the regulatory gene tofM and quorum sensing-independent modulation pathways controlled by QsmR as well as pH-dependent regulation mediated by the membrane protein DbcA [55,56]. These results suggest that BD_21g may employ multiple regulatory mechanisms (such as temperature-dependent, QsmR-mediated, and pH-dependent regulation) to produce toxoflavin in a manner that is distinct from other virulent *B. glumae* strains, which are mainly mediated by the canonical quorum sensing system for pathogenesis. To further investigate the diversity of toxin biosynthetic gene expression in *Burkholderia* species, the presence and sequence identity of the tox operons between the genomes of BD_21g (*B. glumae*) and BDBgla132A (*B. gladioli*) was evaluated. The biosynthetic genes (*toxABCDE*) showed particularly high identity: *toxB* exhibited the highest identity at 98.11%, followed by *toxC* at 97.51%. The transport genes (*toxFGHI*) maintained high sequence identity, with *toxH* reaching 97.48%. This elevated sequence identity indicates that the core toxoflavin biosynthetic and transport machinery remains functionally equivalent between *B. gladioli* and *B. glumae*, supporting the critical role of this toxin in plant pathogenesis [15,52].

According to lipase activity assays, all studied *Burkholderia* strains produced lipase, with BD_21g (*B. glumae*) and *B. gladioli* (BDBgla132A) exhibiting significantly higher activity. RT-qPCR analyses revealed that BD_21g exhibits increased expression of lipase-encoding genes over *B. gladioli* BDBgla132A. The expression of *lipA* and *lipB* genes was elevated by 2.4- and 4-fold, respectively, indicating an active lipid-hydrolysis process that breaks down host membranes to release nutrients. These findings are consistent with prior studies that implicated mutations in the *lipAB* operon promoter region in elevated lipase expression and secretion [57]. Sequence comparison of the lipase-encoding genes (*lipA*/*lipB*) between *B. gladioli* BDBgla132A and BD_21g (*B. glumae*) uncovered variable levels of conservation: *lipA* maintained substantial identity at 88.55% while *lipB* exhibited lower sequence identity at 80.71%. Functional extracellular activity was confirmed by in *vitro* lipase assays with model substrates, indicating that *lipA* and *lipB* encode secreted enzymes capable of hydrolyzing lipid esters and supporting their nutrient acquisition role [19]. Overall, these data support the importance of lipase as a multifaceted virulence factor, with conserved gene sequences and confirmed extracellular enzyme activity, making it a potent therapeutic target for disease control strategies.

All the *Burkholderia* strains analyzed with a qualitative pectate gel assay were confirmed to secrete polygalacturonase [39], while quantification using the Bernfeld method [41] showed that polygalacturonic acid induced polygalacturonase activity consistent with the enzyme's function of degrading this major structural component of plant cell walls [13]. RT-qPCR analysis showed that *pehA* and *pehB* transcript levels in BD_21g were 1.9-fold and 2.0-fold lower than in BDBgla132A, suggesting differential regulation of polygalacturonase production in response to plant cell wall degradation requirements [26]. Comparative sequence analysis of BD_21g (*B. glumae*) and *B. gladioli* (BDBgla132A) revealed that polygalacturonase-encoding genes (*pehA*/*pehB*) shared moderate to high sequence identity between both strains: *pehA* displayed 84.53%, whereas *pehB* exhibited greater identity (87.35%). In *B. cepacia*, the *pehA* gene plays a role in the breakdown of onion bulbs tissues and is implicated in onion rot pathogenicity. [26,58]. Polygalacturonases encoded by *pehA*/*pehB* degrade plant cell wall pectin and represent established virulence factors in *Burkholderia*-mediated host tissue maceration [13]. The similarity of these genes across both species with substantial sequence identity underscores their pivotal role in plant tissue maceration and disease progression. These findings have implications for their virulence system and host specificity. It would be interesting to explore further how environmental conditions, particularly temperature, pH, and pectin concentration, influence *pehA* and *pehB* expression in both species. In addition, determining the exact contribution of polygalacturonase activity to virulence across multi-host plants would be key.

All studied *Burkholderia* strains exhibited swarming motility on 0.5% semi-solid LB medium. However, the motility capacity was strain-dependent, with BDBgla132A displaying the highest motility, followed by BDBgla136A, BDBgla136A, BDBgla138A, and BD_21g. In plant-pathogen interactions, swarming motility is vital for surface colonization and, potentially, systemic dissemination during infection [15,23]. In *B. glumae*, swarming motility (a flagella-driven social

 doi:10.20944/preprints202601.1111.v2

movement of differentiated cells) is regulated by quorum sensing and acyl-homoserine lactone (AHL) signaling molecules and requires the use of rhamnolipid to spread the cells on an agar surface [59]. Quantitative PCR revealed that flagellar regulatory genes *flhC* and *flhF* were expressed at 2.4- and 3.8-fold lower levels in BD_21g relative to BDBgla132A, aligning with the enhanced motility phenotype observed in the latter strain. Different regulators are hypothesized to influence this phenotype. Chemotaxis and flagellar genes displayed complex sequence identity patterns with functional implications for motility and virulence. Core chemotaxis genes (*cheA, cheB, cheD, cheW, cheY, cheY1* and *cheZ*) showed high identity (80.80–97.22%), while the *cheR* deletion in *B. gladioli* BDBgla132A suggests divergent regulatory mechanisms. Flagellar biosynthesis genes (*flhA–flhG*) exhibited high identity (84.39–96.72%), although *fliD* displayed the lowest identity (66.92%). The absence of *motB* and the chemotactic receptor (*tsr*) in BDBgla132A, coupled with the retention of *motA* (96.5%), indicates species-specific adaptations in flagellar function that may influence tissue colonization strategies. These observations are consistent with pan-genome analysis of *B. gladioli*, in which chemotaxis and flagellum-dependent motility are annotated among core functional categories conserved across strains [60]. Motility systems may have evolved to occupy different ecological niches, but the precise role of swarming in BPB-related pathogenesis remains poorly understood. Mutant analyses and *in planta* colonization studies will be required to determine whether differential flagellar gene organization directly influences virulence during rice infection.

Hypersensitivity assays were conducted on tobacco leaves (*Nicotiana tabacum* L.) to assess the functionality of the type III secretion system (T3SS). All *Burkholderia* isolates induced rapid necrotic lesions within 48 hours. The rapid development of necrotic lesions triggered by strains BDBgla132A and BD_21g within 48 hours indicates the functionality of an active type III secretion system (T3SS), confirming earlier reports on the critical requirement of hrp-encoded T3SS components for the delivery of effector proteins into host cells [27]. The isolates' ability to elicit a hypersensitive response (HR) aligns with their dual role in promoting disease in susceptible hosts and in activating plant resistance in resistant hosts, both of which are hallmark functions of intact *hrp* gene clusters [28].

This study investigated the evolutionary relationships and distribution of virulence-associated genes in *B. glumae* and *B. gladioli*. Phylogenetic analyses of key virulence factors, including genes involved in toxoflavin biosynthesis, lipase production, polygalacturonase activity, and flagellar function, revealed that many of these genes are conserved between the two species. Nonetheless, we also noted considerable divergence in some genes, including those involved in motility and chemotaxis. For instance, BD_21g (*B. glumae*) retains some genes related to motility that are absent in *B. gladioli* BDB132A suggesting loss of particular genes during the evolution of *B. gladioli*.

5. Conclusions

In conclusion, the study characterizes *Burkholderia* strains responsible for BPB in Bangladesh and conclusively establishes *B. gladioli* as the predominant pathogen and *B. glumae* as another cause of the disease. Using phenotypic, molecular, and transcriptomic methodologies, precise virulence mechanisms in both species have been identified. Notably, *B. glumae* and *B. gladioli* employ differential virulence strategies: *B. glumae* predominantly utilizes toxoflavin and lipase to target rice, whereas *B. gladioli* rely on pectinolytic enzymes and flagellar systems for pathogenicity. The results of the onion bulb disease model assay, which provides a simple, rapid, and reliable alternative to rice panicle assays, accurately correlate with the severity of rice panicle disease and can be utilized to quickly differentiate between the two pathotypes. Genomic analyses indicate that orthologous virulence genes are preserved within species but have diverged across species. *B. glumae* and *B. gladioli* have evolved distinct specialized strategies to promote their exploitation of rice-growing regions in South and Southeast Asia, representing divergent evolutionary solutions to rice pathogenesis. Additional research using environmentally relevant conditions for tropical rice ecosystems, in combination with targeted mutagenesis and *in planta* colonization studies, will be needed to further advance understanding of the functional importance of individual virulence factors in the progression of BPB disease.

 doi:10.20944/preprints202601.1111.v2

Supplementary Materials: The following supporting information can be downloaded at: Preprints.org. **Table S1:** List of *Burkholderia* isolates collected from 20 districts across Bangladesh; **Table S2:** Primers used for real-time RT- qPCR; **Table S3:** Sequence identity of virulence-associated genes between *B. gladioli* BDBgla132A and *B. glumae* BD_21g compared to *B. cepacia*.

Authors' Contributions: MNU was involved in securing funding, conceiving and designing the study, conducting molecular identification, performing statistical analyses, generating visualizations, and drafting the manuscript. DAP contributed to securing funding for whole genome analyses and drafting the manuscript, and designed and supervised whole genome sequencing of *B. gladioli*. IAP contributed to securing funding for whole genome analyses and assisted in whole genome data analyses. MRI designed and supervised entire study including the field isolate collection, molecular identification, and whole genome sequencing of *B. glumae*, and also contributed to drafting and editing the manuscript. RA assisted in field survey and in statistical data analysis. FK contributed to statistical and molecular data analysis. MHH, PS, UAM and MS assisted with laboratory work, including DNA extraction and PCR detection. MIH helped with statistical data analysis. MSI and FH participated in field survey and data collection. All authors have read and approved the final version of the manuscript.

Funding: This project was partially supported by a Science and Technology Fellowship Trust from the Ministry of Science and Technology, Government of the People's Republic of Bangladesh and by a Nevada INBRE Scientific Core Service Award, funded by grant GM103440 from the National Institute of General Medical Sciences.

Institutional Review Board Statement: Not Applicable.

Informed Consent Statement: Not Applicable.

Data Availability Statement: Research data generated in this study are available from the corresponding author upon reasonable request.

Acknowledgments: The authors express their sincere gratitude to the local personnel of the Department of Agricultural Extension, Ministry of Agriculture, Government of the People's Republic of Bangladesh, for their invaluable support in facilitating field sample collection.

Conflicts of interest: The authors declare that they have no competing interests.:

Abbreviations:

BLASTp: Basic Local Alignment Search Tool-protein

BPB: Bacterial Panicle Blight

Bcc: *Burkholderia cepacia* complex

CDD: Conserved Domain Database

DS: Disease Severity

HR: Hyper-sensitive response

S-PG: Sucrose-Peptone-Glutamate

KBA: King’s B agar

LB: Luria Broth or Luria–Bertani

PGA: Polygalacturonic acid

PCR: Polymerase Chain Reaction

RT-qPCR: Reverse Transcription quantitative PCR

T3SS: type III secretion system

NCBI: National Center for Biotechnology Information

 doi:10.20944/preprints202601.1111.v2

References

1. Islam, M.R.; Jannat, R.; Protic, I.A.; Happy, M.N.A.; Samin, S.I.; Mita, M.M.; et al. First report of bacterial panicle blight in rice caused by *Burkholderia gladioli* in Bangladesh. *Plant Dis.* **2023**, 107, 2837, doi:10.1094/PDIS-02-23-0229-PDN.
2. Ham, J.H.; Melanson, R.A.; Rush, M.C. *Burkholderia glumae*: next major pathogen of rice? *Mol Plant Pathol.* **2011**, 12, 329–39, doi:10.1111/j.1364-3703.2010.00676.x.
3. Nandakumar, R.; Shahjahan, A.K.M.; Yuan, X.L.; Dickstein, E.R.; Groth, D.E.; Clark, C.A.; et al. *Burkholderia glumae* and *B. gladioli* cause bacterial panicle blight in rice in the southern United States. *Plant Dis.* **2009,** 93, 896–905, doi:10.1094/PDIS-93-9-0896. PMID: 30754532.
4. Cui, Z.Q.; Zhu, B.; Xie, G.L.; Li, B.; Huang, S.W. Research status and prospect of *Burkholderia glumae*, the pathogen causing bacterial panicle blight. *Rice Sci.* **2016**, 23, 111–18, doi:10.1016/j.rsci.2016.01.007.
5. Goto, K.; Ohata, K. New bacterial disease of rice (brown stripe and grain rot). *Ann Phytopathol Soc Jpn.* **1956**, 21, 46–47.
6. Zhou, X.G. Sustainable strategies for managing bacterial panicle blight in rice. In Protecting Rice Grains in the Post-Genomic Era; Jia, Y., Ed.; IntechOpen: London, UK, **2019**; doi:10.5772/intechopen.84882.
7. Uddin, M.N.; Protic, I.A.; Tushar, A.S.M.; Hasan, M.; Saha, P.; Singha, U.R.; et al. First report of *Burkholderia glumae* causing bacterial panicle blight in rice in Bangladesh. *Plant Dis.* **2025**, 109, 491, doi:10.1094/PDIS-04-24-0904-PDN.
8. Schaad, N.W.; Jones, J.B.; Chun, W. Laboratory Guide for Identification of Plant Pathogenic Bacteria, 3rd ed.; American Phytopathological Society Press: St. Paul, MN, USA, 2001.
9. Maeda, Y.; Shinohara, H; Kiba, A.; Ohnishi, K.; Furuya, N.; Kawamura, Y.; Ezaki, T.; Hikichi, Y. Phylogenetic study and multiplex PCR-based detection of *Burkholderia plantarii*, *Burkholderia glumae* and *Burkholderia gladioli* using gyrB and rpoD sequences. Int. J. Syst. Evol. Microbiol. **2006**, 56, 1031–1038, doi:10.1099/ijs.0.64184-0.
10. Nandakumar, R.; Rush, M.; Shahjahan, A.K.M.; O'Reilly, K.; Groth, D. Bacterial panicle blight of rice in the southern United States caused by *Burkholderia glumae* and *B. gladioli*. Phytopathology **2005**, 95, S73.
11. Shahjahan, A.K.M.; Rush, M.C.; Groth, D.E.; Clark, C.A. Panicle blight. *Rice J.* **2000**, 15, 26–29.
12. Aviv, Y.; Gal-Mor, O. Real-time reverse transcription PCR as a tool to study virulence gene regulation in bacterial pathogens. Methods Mol. Biol. **2018**, 1734, 23–32, doi:10.1007/978-1-4939-7604-1_3.
13. Degrassi, G.; Devescovi, G.; Kim, J.; Hwang, I.; Venturi, V. Identification, characterization and regulation of two secreted polygalacturonases of the emerging rice pathogen *Burkholderia glumae*. *FEMS Microbiol. Ecol.* **2008**, *65*, 251–262, doi: 10.1111/j.1574-6941.2008.00516.x.
14. Kang, Y.; Kim, J.; Kim, S.; Kim, H.; Lim, J.Y.; Kim, M.; et al. Proteomic analysis of the proteins regulated by HrpB from the plant pathogenic bacterium Burkholderia glumae BGR1. Proteomics 2008, 8, 106–121, doi:10.1002/pmic.200700244.
15. Kim, J.; Kim, J.G.; Kang, Y.; Jang, J.Y.; Jog, G.J.; Lim, J.Y.; Kim, S.; Suga, H.; Nagamatsu, T.; Hwang, I. Quorum sensing and the LysR-type transcriptional activator ToxR regulate toxoflavin biosynthesis and transport in *Burkholderia glumae*. *Mol. Microbiol.* **2004**, *54*, 921–934, doi:10.1111/j.1365-2958.2004.04338.x.
16. Suzuki, F.; Sawada, H.; Azegami, K.; Tsuchiya, K. Molecular characterization of the tox operon involved in toxoflavin biosynthesis of *Burkholderia glumae*. *J Gen Plant Pathol.* **2004**, 70, 97–107, doi:10.1007/s10327-003-0096-1.
17. Matsuda, I.; Sato, Z. Relations between pathogenicity and pigment productivity in the causal agent of bacterial grain rot of rice. *Ann. Phytopathol. Soc. Jpn.* **1988**, 54, p. 378.
18. Kim, J.; Oh, J.; Choi, O.; Kang, Y.; Kim, H.; Goo, E.; Ma, J.; Nagamatsu, T.; Moon, J.S.; Hwang, I. Biochemical evidence for ToxR and ToxJ binding to the tox operons of *Burkholderia glumae* and mutational analysis of ToxR. *J Bacteriol.* **2009**, 191, 4870–4878, doi:10.1128/jb.01561-08.
19. Frenken, L.G.; de Groot, A.; Tommassen, J.; Verrips, C.T. Role of the *lipB* gene product in the folding of the secreted lipase of *Pseudomonas glumae*. *Mol Microbiol.* **1993**, 9, 579–89, doi:10.1111/j.1365-2958.1993.tb01719.x.
20. El Khattabi, M.; Van Gelder, P.; Bitter, W.; Tommassen, J. Role of the lipase-specific foldase of *Burkholderia glumae* as a steric chaperone. *J Biol Chem.* **2000**, 275, 26885–91, doi:10.1074/jbc.m003258200.

 doi:10.20944/preprints202601.1111.v2

21. Davey, M.E.; O'Toole, G.A. Microbial biofilms: From ecology to molecular genetics. *Microbiol. Mol. Biol. Rev*. **2000**, 64, 847–867, doi:10.1128/mmbr.64.4.847-867.2000.
22. Kim, J.; Kang, Y.; Choi, O.; Jeong, Y.; Jeong, J.E.; Lim, J.Y.; et al. Regulation of polar flagellum genes is mediated by quorum sensing and FlhDC in *Burkholderia glumae*. *Mol Microbiol.* **2007**, 64, 165–179, doi:10.1111/j.1365-2958.2007.05646.x.
23. Jang, M.S.; Goo, E.; An, J.H.; Kim, J.; Hwang, I. Quorum sensing controls flagellar morphogenesis in Burkholderia glumae. *PLoS One* **2014**, 9, e84831, doi:10.1371/journal.pone.0084831.
24. Abbott, D.W.; Boraston, A.B. Structural biology of pectin degradation by Enterobacteriaceae. *Microbiol Mol Biol Rev.* **2008**, 72, 301–16, doi:10.1128/MMBR.00038-07.
25. Huang, Q.; Allen, C. An exo-poly-alpha-D-galacturonosidase, PehB, is required for wild-type virulence of *Ralstonia solanacearum* on tomato. *J Bacteriol.* **1997**, 179, 7369–78, doi:10.1128/jb.179.23.7369-7378.1997.
26. Gonzalez, C.F.; Pettit, E.A.; Valadez, V.A.; Provin, E.M. Mobilization, cloning, and sequence determination of a plasmid-encoded polygalacturonase from a phytopathogenic *Burkholderia* (*Pseudomonas*) *cepacia*. *Mol Plant Microbe Interact.* **1997**, 10, 840–51, doi:10.1094/mpmi.1997.10.7.840.
27. Cornelis, G.R.; Van Gijsegem, F. Assembly and function of type III secretory systems. *Annu Rev Microbiol.* **2000**, 54, 735–74, doi:10.1146/annurev.micro.54.1.735.
28. Lindgren, P.B. The role of *hrp* genes during plant-bacterial interactions. *Annu Rev Phytopathol.* **1997**, 35, 129–52, doi:10.1146/annurev.phyto.35.1.129.
29. Protic, I.A.; Uddin, M.N.; Tushar, A.S.M.; Auyon, S.T.; Alvarez-Ponce, D.; Islam, M.R. First complete genome sequence of a bacterial panicle blight-causing pathogen, *Burkholderia glumae*, isolated from symptomatic rice grains from Bangladesh. *BMC Genomic Data* **2024**, 25, 73, doi:10.1186/s12863-024-01255-5.
30. Protic, I.A.; Uddin, M.N.; Gorzalski, A.; et al. Comparative genomic analyses shed light on the introduction routes of rice-pathogenic *Burkholderia gladioli* strains into Bangladesh. *BMC Genomics* **2026,** 27, 121, doi:10.1186/s12864-025-12430-y.
31. Mirghasempour, S.A.; Huang, S.; Xu, W.; et al. First report of *Burkholderia gladioli* causing rice panicle blight and grain discoloration in China. *Plant Dis.* **2018**, 102, 2635, doi:10.1094/PDIS-05-18-0758-PDN.
32. Tsushima, S.; Wakimoto, S.; Mogi, S. Selective medium for detecting Pseudomonas glumae Kurita et Tabei, the causal bacterium of grain rot of rice. *Ann. Phytopathol. Soc. Jpn.* **1986**, 52, 253–259, doi:10.3186/jjphytopath.52.253.
33. Echeverri-Rico, J.; Restrepo, S.; Guerra-Sierra, A.; Escobar, C. Understanding the complexity of disease–climate interactions driving bacterial panicle blight of rice caused by *Burkholderia glumae* in Colombia. *PLoS One* **2021**, 16, e0252061, doi:10.1371/journal.pone.0252061.
34. Jacobs, J.L.; Fasi, A.C.; Ramette, A.; Smith, J.J.; Hammerschmidt, R.; et al. Identification and onion pathogenicity of *Burkholderia cepacia* complex isolates from the onion rhizosphere and onion field soil. *Appl Environ Microbiol.* **2008**, 74, 3121–9, doi:/10.1128/aem.01941-07.
35. Furuya, N.; Iiyama, K.; Ueda, Y.; Matsuyama, N. Reaction of Tobacco and Rice Leaf Tissue Infiltrated with *Burkholderia glumae* or *B. gladioli*. *J. Fac. Agric. Kyushu Univ.* **1997**, 42, 43–51, doi:10.5109/24190.
36. Jung, W.-S.; Lee, J.; Kim, M.-I.; Ma, J.; Nagamatsu, T.; Goo, E.; Kim, H.; Hwang, I.; Han, J.; Rhee, S. Structural and Functional Analysis of Phytotoxin Toxoflavin-Degrading Enzyme. *PLoS ONE* **2011**, *6*, e22443, doi:10.1371/journal.pone.0022443.
37. Sierra, G. A simple method for the detection of lipolytic activity of micro-organisms and some observations on the influence of the contact between cells and fatty substrates. Antonie Van Leeuwenhoek **1957**, 23, 15–22, doi:10.1007/BF02545855.
38. Winkler, U.K.; Stuckmann, M. Glycogen, hyaluronate, and some other polysaccharides greatly enhance the formation of exolipase by *Serratia marcescens*. *J Bacteriol.* **1979**, 138, 663–70, doi:10.1128/jb.138.3.663-670.1979.
39. Starr, M.P.; Chatterjee, A.K.; Starr, P.B.; Buchanan, G.E. Enzymatic degradation of polygalacturonic acid by Yersinia and Klebsiella species in relation to clinical laboratory procedures. J. Clin. Microbiol. 1977, 6, 379–386, doi:10.1128/jcm.6.4.379-386.1977.
40. Sambrook, J.; Fritsch, E.F.; Maniatis, T. *Molecular Cloning: A Laboratory Manual*, 2nd ed.; Cold Spring Harbor Laboratory Press: Cold Spring Harbor, NY, USA, **1989**.

 doi:10.20944/preprints202601.1111.v2

41. Bernfeld, P. Amylase, α and β. In Methods in Enzymology; Colowick, S.P., Kaplan, N.O., Eds.; Academic Press: New York, NY, USA, **1955**; Volume 1, pp. 149–158, doi:10.1016/0076-6879(55)01021-5.
42. Lee, J.Y.; Park, J.W.; Kim, S.Y.; Park, I.M.; Seo, Y.S. Differential regulation of toxoflavin production and its role in the enhanced virulence of *Burkholderia gladioli*. *Mol. Plant Pathol*. **2016**, 17, 65–76, doi:10.1111/mpp.12262.
43. Livak, K.J.; Schmittgen, T.D. Analysis of relative gene expression data using real-time quantitative PCR and the $2^{-\Delta\Delta CT}$ method. Methods **2001**, 25, 402–408, doi:10.1006/meth.2001.1262.
44. Kumar, S.; Stecher, G.; Suleski, M.; Sanderford, M.; Sharma, S.; Tamura, K. MEGA12: Molecular evolutionary genetic analysis version 12 for adaptive and green computing. Mol. Biol. Evol. **2024**, 41, msae263, doi:10.1093/molbev/msae263
45. Tamura, K.; Nei, M. Estimation of the number of nucleotide substitutions in the control region of mitochondrial DNA in humans and chimpanzees. Mol. Biol. Evol. **1993**, 10, 512–526, doi:10.1093/oxfordjournals.molbev.a040023.
46. Jungkhun, N.; Gomes de Farias, A.R.; Watcharachaiyakup, J.; Kositcharoenkul, N.; Ham, J.H.; Patarapuwadol, S. Phylogenetic characterization and genome sequence analysis of *Burkholderia glumae* strains isolated in Thailand as the causal agent of rice bacterial panicle blight. *Pathogens* **2022**, 11, 676, doi:10.3390/pathogens11060676.
47. Luo, J.; Xie, G.; Li, B.; Xu, L. First Report of *Burkholderia glumae* Isolated from Symptomless Rice Seeds in China. *Plant Dis.* **2007**, *91*, 1363, doi:10.1094/pdis-91-10-1363b.
48. Chien, C.C.; Chang, Y.C. The Susceptibility of Rice Plants at Different Growth Stages and of 21 Commercial Rice Varieties to *Pseudomonas glumae*. *J. Agric. Res. China* **1987**, 36, 302–310.
49. Tsushima, S.; Naito, H.; Koitabashi, M. Population Dynamics of *Pseudomonas glumae*, the Causal Agent of Bacterial Grain Rot of Rice, on Leaf Sheaths of Rice Plants in Relation to Disease Development in the Field. *Jpn. J. Phytopathol.* **1996**, 62, 108–113, doi:10.3186/JJPHYTOPATH.62.108.
50. Burkholder, W.H. Sour skin, a bacterial rot of onion bulbs. *Phytopathology* **1950**, 40, 115–117.
51. Sotokawa, M.; Takikawa, Y. Occurrence of bacterial rot of onion bulbs caused by *Burkholderia cepacia* in Japan. *J. Gen. Plant Pathol.* **2004**, 70, 348–352, doi:10.1007/s10327-004-0159-y.
52. Karki, H.S.; Shrestha, B.K.; Han, J.W.; Groth, D.E.; Barphagha, I.K.; Rush, M.C.; Melanson, R.A.; Ham, J.H. Diversities in virulence, antifungal activity, pigmentation and DNA fingerprint among strains of *Burkholderia glumae*. *PLoS ONE* 2012, 7, e45376, doi:10.1371/journal.pone.0045376.
53. Sato, Z.; Koiso, Y.; Iwasaki, S.; Matsuda, I.; Shirata, A. Toxins produced by *Pseudomonas glumae*. *Ann. Phytopathol. Soc. Jpn.* **1989**, 55, 353–356.
54. Iiyama, K.; Furuya, N.; Takanami, Y.; Matsuyama, N. A role of phytotoxin in virulence of *Pseudomonas glumae* Kurita et Tabei. *Ann. Phytopathol. Soc. Jpn.* **1995**, 61, 470–476, doi:10.3186/jjphytopath.61.470.
55. Chen, R.; Barphagha, I.K.; Karki, H.S.; Ham, J.H. Dissection of Quorum-Sensing Genes in *Burkholderia glumae* Reveals Non-Canonical Regulation and the New Regulatory Gene *tofM* for Toxoflavin Production. *PLoS ONE* **2012**, 7, e52150, doi:10.1371/journal.pone.0052150.
56. Iqbal, A.; Nwokocha, G.; Tiwari, V.; Barphagha, I.K.; Grove, A.; Ham, J.H.; Doerrler, W.T. A membrane protein of the rice pathogen *Burkholderia glumae* required for oxalic acid secretion and quorum sensing. *Mol. Plant Pathol.* **2023**, 24, 1400–1413. https://doi.org/10.1111/mpp.13376
57. Knapp, A.; Voget, S.; Gao, R.; Milewski, S.; Jaeger, K.E.; Hausmann, S. Mutations improving production and secretion of extracellular lipase by *Burkholderia glumae* PG1. *Appl. Microbiol. Biotechnol.* **2016**, 100, 1265–1273, doi:10.1007/s00253-015-7041-z.
58. Aguilar, C.; Bertani, I.; Venturi, V. Quorum-sensing system and stationary-phase sigma factor (rpoS) of the onion pathogen *Burkholderia cepacia* genomovar I type strain, ATCC 25416. *Appl. Environ. Microbiol.* **2003**, *69*, 1739–1747, doi:10.1128/AEM.69.3.1739-1747.2003.
59. Nickzad, A.; Lépine, F.; Déziel, E. Quorum sensing controls swarming motility of *Burkholderia glumae* through regulation of rhamnolipids. PLoS ONE **2015**, 10, e0128509, doi:10.1371/journal.pone.0128509.
60. Lee, H.H.; Kim, J.; Park, H.; Kang, J.; Lee, J. Pan-genome analysis reveals host-specific functional diversification in *Burkholderia gladioli*. Microorganisms **2021**, 9, 1062, doi:10.3390/microorganisms9061123.

 doi:10.20944/preprints202601.1111.v2